JPL Publication 97-16

LISA Mission Concept Study

Laser Interferometer Space Antenna For the Detection and Observation of Gravitational Waves

W. M. Folkner
Jet Propulsion Laboratory

P. L. Bender
R. T. Stebbins
University of Colorado

March 2, 1998

Jet Propulsion Laboratory
California Institute of Technology

The research described in this publication was carried out by the Jet Propulsion Laboratory, California Institute of Technology, under a contract with the National Aeronautics and Space Administration.

FOREWORD

Mission concept studies for a space-borne gravitational wave observatory began at the University of Colorado in the 1970s. Starting in 1980, the studies centered on the concept of a constellation of spacecraft in a heliocentric orbit 1 AU (150×10^6 km) from the Sun and 20° to 60° behind the Earth (which is 0.34–1 AU or $52–150 \times 10^6$ km). The heliocentric orbit provides for reasonably constant distances between spacecraft and a stable environment that gives low noise forces on the test mass. The Laser Interferometer Space Antenna (LISA) mission was proposed in May 1993, by a team of United States and European scientists as a joint NASA/ESA (National Aeronautics and Space Administration/European Space Agency) mission for ESA's M3 (third medium) mission opportunity. It was chosen by ESA instead for an Assessment Study as a possible ESA-only mission. The ESA-led study indicated that, without NASA participation, LISA was too expensive for the M3 mission opportunity, and thus could not be selected as the M3 mission.

In addition to the M3 opportunity, LISA was suggested in October 1993, as a candidate for a Cornerstone mission under ESA's proposed new Horizon 2000 Plus program. A Technical Assessment of LISA as a Cornerstone mission was carried out by ESA in September. The ESA Space Science Advisory Committee (SSAC) met in October 1994, and recommended that ESA ask each of the member states to increase their contributions after the year 2000 so that LISA could be included as one of three new Cornerstone missions, with a launch date of 2016 or sooner. The requested ESA budget increase was not approved. ESA's SSAC later confirmed their intention to fly the LISA mission but the timetable remains very uncertain.

In addition to the schedule uncertainty, the ESA cost estimates were very high. The cost of the six-spacecraft Cornerstone mission was estimated, in a very preliminary manner, at $960M exclusive of the payload. The six-spacecraft mission was also near the limit of the large Ariane 5 launch vehicle.

In order to reduce the mission cost, the science team studied an alternative configuration using only three spacecraft. Each of the new spacecraft would replace a pair of spacecraft at the vertices of the triangular configuration, with essentially two instruments in each spacecraft. The three spacecraft would maintain all of the science capabilities of the six-spacecraft Cornerstone mission and would include redundancy in the sense that no single failure would end the mission. In the case of the failure of one instrument, the mission would degrade gracefully into a two-arm interferometer, rather than the preferred three-arm mission, which would still provide much of the expected science return.

A candidate configuration of the three-spacecraft mission was developed by the science team, with the goal of being able to launch the three spacecraft on a Delta-II. The three-spacecraft LISA mission was analyzed by a mission design team (Team-X) during 14–18 January 1997. The purpose of the study was to assist the science team, represented by P.L. Bender and R.T. Stebbins (University of Colorado), and W.M. Folkner (JPL), in defining the necessary spacecraft subsystems and in designing a propulsion module capable of delivering the LISA spacecraft into the desired orbit. The team also generated a grass-roots cost estimate based on experience with similar subsystem designs developed at JPL.

The result of the Team X study was that it appeared feasible to fly the three-spacecraft LISA mission on a single Delta-II 7925H launch vehicle by utilizing a propulsion module based on a

solar-electric propulsion, and with spacecraft subsystems expected to be available by a 2001 technology cut-off date. The total estimated mission cost is $465M (FY 1997 $), including development, construction, launch vehicle, and mission operations.

This report includes the results of the Team-X study. For the use of outside readers, the science team has included introductory material and re-arranged the elements of the Team-X study results to reflect the choice of solar electric propulsion for delivery of the LISA spacecraft to their final orbits as the new baseline.

For LISA, Team-X was comprised of the following representatives:

Subsystem	Team Member
Study Leader	Richard Bennett
Science	Steve Edberg
Thermal	Bob Miyake
Structures	Gerhard Klose and Moktar Salama
Attitude Determination and Control System	Ed Mettler and Ed Swenka
Command and Data System	Shirley Peak
Systems	Bob Rowley
Mission Design	Ted Sweetser
Ground Systems	Mark Rokey
Cost	Leigh Rosenberg
Telecom-System	Anil Kantak
Telecom-Hardware	Faiza Lansing
Power	Steve Dawson
Propulsion	Ron Klemetson
Instruments	Jim Anderson
Documentarian	Larry Palkovic
Computer Tool Support	Joseph Aguilar and Glenn Law

The results of the Team-X study are intended to demonstrate feasibility and to estimate the equipment, mass, and cost required to implement the science team's mission. The design documented herein is intended to be a representative solution, developed with a minimum expenditure of workforce and time. As a result, this representative solution has not been optimized and may be incomplete or inaccurate. It is strongly recommended that a more detailed study be completed before final implementation decisions are made.

TABLE OF CONTENTS

List of Figures

List of Tables

SECTION 1—INTRODUCTION

The goal of LISA (Laser Interferometer Space Antenna) is to detect and study low-frequency astrophysical gravitational radiation. The data will be used for research in astrophysics, cosmology, and fundamental physics. LISA is designed to detect the gravitational radiation from regions of the universe that are strongly relativistic, e.g., in the vicinity of black holes. The types of exciting astrophysical sources potentially visible to LISA include extra-galactic massive black hole binaries at cosmological distances, binary systems composed of a compact star and a massive black hole, galactic neutron star-black hole binaries, and background radiation from the Big Bang. LISA will also observe galactic binary systems, which are statistically known to exist. Observation of these galactic binaries will provide strong verification of the instrument performance.

Gravitational waves are one of the fundamental building blocks of our theoretical picture of the universe. There is clear indirect evidence of their existence. The best example is the binary pulsar PSR 1913+16, a system that has been followed in its evolution for almost 20 years [Taylor and Weisberg 1989]. The binary system is losing energy at exactly the rate predicted by general relativity due to the emission of gravitational waves. However, direct detection of gravitational radiation signals has not yet been achieved.

The effect of a gravitational wave passing through a system of free test masses is to create a strain in space that changes distances between the masses. The main problem is that the relative length change due to the passage of a gravitational wave is exceedingly small. Several ground-based laser interferometers with arm lengths of several kilometers are now either proposed [Hough et al. 1989; Danzmann et al. 1992], approved [Bradaschia et al. 1990], or under construction [Abramovici et al. 1992]. These km-size ground-based laser interferometers will be sensitive to gravitational waves at frequencies of tens to thousands of hertz. It is likely that they will go into operation soon after the end of this decade, aiming at the first direct detection of gravitational radiation.

Ground-based detectors are expected to provide fundamental information about coalescing binary stars, the core collapse of supernova events, and the distribution and properties of pulsars, but they will always be limited to frequencies above 1 Hz due to the unshieldable background of Newtonian gravity variations on the Earth. Only space-borne detectors can open the low-frequency window to the universe for gravitational waves, where low-frequency refers to the frequency range 0.1 mHz to 1 Hz. This frequency range is likely to contain the astrophysically most interesting sources. Only in the low-frequency range can the emission associated with massive black holes in galactic nuclei be observed. This capability led the ad hoc Committee on Gravitation Physics and Astronomy of the NASA Astrophysics Division in 1990 to recommend technology development for a laser gravitational wave mission as the first priority in its field.

The LISA mission (Fig. 1-1) will comprise three spacecraft located 5×10^6 km apart forming an equilateral triangle. The spacecraft orbits are selected such that the triangular formation is maintained throughout the year with the triangle appearing to rotate about the center of the formation once per year. The center of the triangle formation will be in the ecliptic plane 1 AU (150×10^6 km) from the Sun and 20° behind (52×10^6 km) the Earth. LISA will detect gravitational wave strains down to a level of order 10^{-23} in one year of observation time by

measuring the fluctuations in separation between shielded test masses located within each spacecraft.

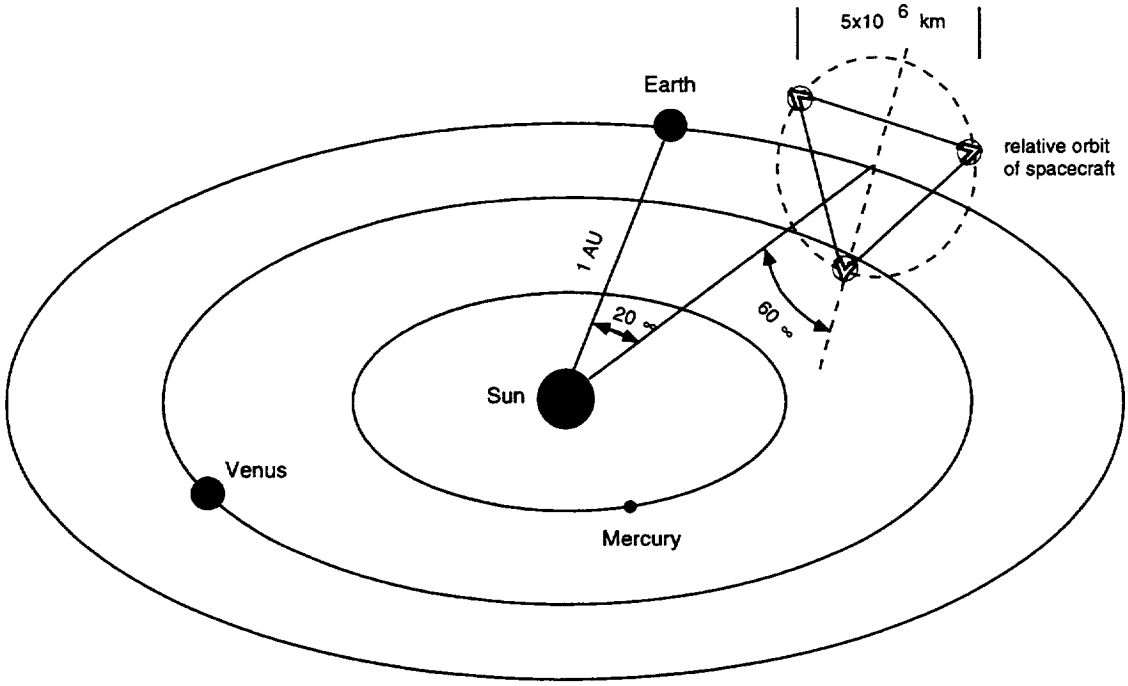

Figure 1-1 Schematic diagram of the LISA configuration. Three spacecraft form an equilateral triangle with sides 5 million km in length. The plane of the triangle is tilted by 60° out of the ecliptic. The two optical assemblies on one spacecraft combine with an optical assembly from each of the other two spacecraft to form a Michelson interferometer. The drawing is not to scale.

The measurement will be performed by optical interferometry which determines the phase shift of laser light transmitted between the test masses. Each test mass is shielded from extraneous disturbances (e.g., solar pressure) by the spacecraft in which it is accommodated. Each spacecraft contains two optical assemblies, each of which in turn houses a test mass centered in an optical bench and a 30-cm diameter telescope. Each telescope can act as the vertex of a two-arm interferometer with ends defined by a single optical assembly on each of the other two spacecraft. Of the three possible interferometers, two are independent giving information about both polarizations of received gravitational waves. At each spacecraft, the relative displacements between the spacecraft and the two test masses are measured electrostatically. Micronewton electric thrusters are operated to keep the spacecraft structure centered on the average position of the two test masses. This drag-free operation reduces non-gravitational forces on the test masses to an acceptable level.

Data on the measured distance between the test masses are continuously acquired throughout the mission. Pre-processing of the data is done by the spacecraft computer to remove the laser phase noise and reduce the signal bandwidth. The data are stored in the spacecraft computer memory. The current plan is for the data to be transmitted to Earth every other day. A single 10.5-hour tracking pass of a Deep Space Network (DSN) 34-m antenna would be used to download both science and housekeeping data from each spacecraft.

SECTION 2—SCIENCE OBJECTIVES

The primary objective of the LISA mission, as viewed from a U.S. perspective, is to detect and study in detail gravitational wave signals from sources involving massive black holes. This includes both signals from the terminal stages of binary coalescences, which we will call bursts, and binary signals which are continuous over the observation period. The scientific information obtainable from such sources, both for astrophysics and for testing current predictions of gravitational theory, is enormous. The main issues are whether the bursts occur frequently enough so that a number can be observed over the mission lifetime, and whether the stronger continuous signals can be observed over the instrumental and other noise limitations. Most of the burst signals would be observable with high signal-to-noise ratio out to large red shifts.

Other important objectives also exist. LISA will certainly observe distinguishable signals from thousands of binary systems containing compact stars, and be able to determine the number and distribution of such binaries in our galaxy. The directions to the sources can be determined from the amplitude and phase changes of the signals during the year. At frequencies below about 3 mHz the number of galactic binaries will be large enough to interfere with the observation of some important extragalactic sources. Signals from some known binary systems are also likely to be seen. In addition, a useful search for a continuous spectrum of gravitational radiation generated at early times would be carried out. The expected LISA sensitivity and the signal levels of several expected sources are indicated in Fig. 2-1 and discussed below.

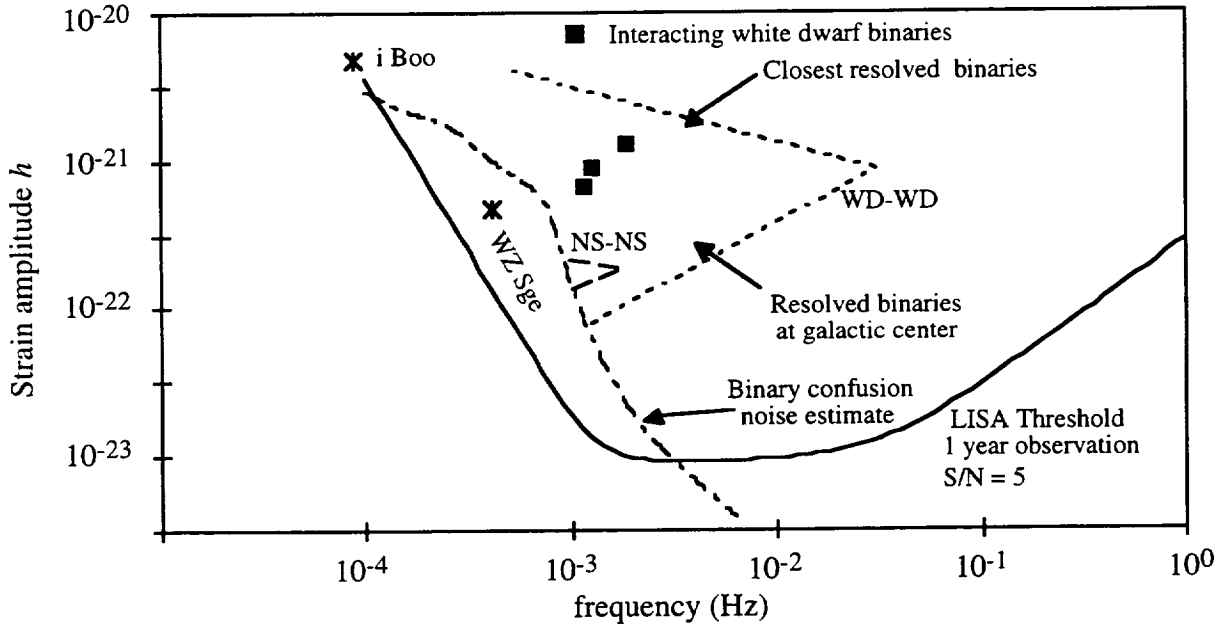

Figure 2-1 LISA sources and sensitivity. The sensitivity curve for LISA (solid line) is for an integration time of 1 year, a signal-to-noise ratio of 5, and an isotropic average over source directions. The lower and upper dashed lines give the expected signal strengths versus frequency for sources at the galactic center and the nearest neutron-star binaries (NS-NS). The chain-dashed line indicates a confusion-limited background due to close white dwarf binaries (WD-WD), at 10% of the upper bound for their numbers. See text for discussions of these and other types of sources.

2.1 ABUNDANCE AND FORMATION OF MASSIVE BLACK HOLES

There now is strong direct evidence for the existence of massive black holes in the nuclei of many galaxies. Probably the best evidence so far is the recent observations of the disk in M87 with the Hubble Space Telescope (HST) [Ford et al. 1994; Harms et al. 1994]. The data reveal the details of both the brightness cusp at the center and the large asymmetric Doppler shifts across the center with resolution unprecedented in ground-based observations.

For galaxies in the Local Group, HST observations of M32 by Lauer et al. [1992] show a brightness cusp in the center that can be interpreted most easily as indicating the presence of a 3×10^6 $M_\odot$ black hole. For M31 the situation is more complicated because the nucleus shows two cusps [Lauer et al. 1993], but the results are consistent with the presence of at least one massive black hole. Since M32 and M31 are two of only four spiral or elliptical galaxies in the Local Group (other than our galaxy) which are as luminous as M32, the statistics are of strong interest. If it turns out that both of these galaxies do indeed contain massive black holes, this would suggest that perhaps 20% to 50% of all spiral and elliptical galaxies above the size of M32 (3×10^9 $M_\odot$) contain such objects.

Another important source of observational information concerning the amount of matter in massive black holes comes from the integrated light of quasars [Soltan 1982; Chokshi and Turner 1992]. From the amount of matter which has to have been fed in to produce the light, at least 3×10^{-5} of all the baryons in the universe are contained in massive black holes.

It is not yet known how supermassive black holes form, although a great deal has been written on this subject. One consideration discussed recently by Haehnelt and Rees [1993]and Rees [1997a, 1997b] is that, in most hierarchical models for formation of structure in the universe, the build-up of structures of galactic size occurs at a time similar to the peak of the quasar activity. They argue that the time scale for the formation of a black hole in a newly forming dark-matter halo is short, and that there need not be a time lag between the formation of a proto-galaxy and the "switching on" of a quasar. If a density concentration of the order of 10^8 $M_\odot$ occurs in a region 1 parsec (3×10^{16} km) across, they conclude that it will have no non-relativistic equilibrium state which can be supported for long, and will collapse to a supermassive black hole.

Another approach taken by Quinlan and Shapiro [1990] is to start from an assumed dense cluster of stars in a galactic nucleus and follow the build-up of 100 $M_\odot$ or larger seed black holes by collisions. The further growth to a supermassive black hole would then be by the types of mechanisms investigated by Duncan and Shapiro [1983]; David, Durisen, and Cohn [1987]; and Murphy, Cohn, and Durisen [1989]. These mechanisms include the feeding of the black hole by tidal disruption of stars, pre-existing gas, and gas from solar winds.

Alternate ways of forming seed black holes of perhaps 10^5 to 10^7 $M_\odot$ (10^{35} to 10^{37} km) have been investigated recently by Umemura, Loeb, and Turner [1993] and by Eisenstein and Loeb [1995]. Umemura et al. include inverse Compton coupling with the microwave background at red shifts above roughly 160 to dissipate angular momentum from partially ionized density fluctuations near the Jeans mass and allow them to collapse. Eisenstein and Loeb consider the statistical distribution of tidal torques for density fluctuations in different regions of proto-galaxies, and they find that the number of such regions having low angular momentum and thus be able to collapse rapidly is large. The estimated density of massive black holes formed by such collapses is comparable with or larger than the density of bright galaxies.

2.2 BINARY SYSTEMS COMPOSED OF TWO MASSIVE BLACK HOLES

A generally recognized way of forming massive black hole binaries (MBH-MBH) is the merger of pre-galactic structures or of galaxies which already contained massive black holes [Roos 1981, 1985a, 1985b; Haehnelt 1994]. The existence of many galaxies today which show evidence of recent mergers is now widely accepted [e.g., Toomre 1977; Roos 1985a, 1985b]. In addition, studies indicate that a substantial fraction of structures in the precursors of rich clusters are likely to have undergone mergers [e.g., Evrard 1994; Hernquist 1994]. Thus, if massive black holes were present before mergers, and if the time necessary for the two massive black holes to come close together by interaction with the star density in the galactic nucleus is short enough, coalescence signals will be produced. The question of the MBH-MBH approach time is being investigated by a number of groups, but it seems likely that it will be less than the Hubble time in most cases.

If we want to estimate the rate of MBH-MBH coalescence events, and we assume that 20% to 50% of spiral and elliptical galaxies today above a certain size contain massive black holes, the crucial question is at what stage of structure formation were the massive black holes produced. If at least moderate-sized massive black holes (10^4 to 10^7 $M_\odot$) were common before the time of most rapid evolution in the precursors of rich clusters, then coalescence rates of a number of events per year seem reasonable. However, since we do not yet know how massive black holes formed, we also do not know when they formed. Thus, it is not possible to estimate an expected event rate. On the other hand, it may be just as difficult to find scenarios with large numbers of massive black holes today which give low event rates as to find ones giving rates of a few per year. It also should be remembered that any massive black hole formation mechanism that can occur at a number of locations in some galaxies can add to the coalescence rate.

LISA should be able to detect MBH-MBH coalescence events involving MBH masses of $M_\odot$ or greater at a distance of 3 Gpc (9×10^{14} km; redshift z~1) and beyond.

If MBH-MBH binary signals are observed, they will provide a large amount of detailed information [e.g., Cutler and Flanagan 1994; Apostolatos 1994]. The number of cycles observed will be typically 10^4, and dynamic effects which modify the phase by even half a cycle with respect to a simple chirped signal can be detected for an S/N as low as 5. This is because the cross-correlation with the theoretical signal will become small, as pointed out particularly by Cutler et al. [1993] for neutron star binaries. The rotation rates of the massive black holes will show up very clearly because of their strong effects on the orbital dynamics. The masses of the two massive black holes and a measure of the red shift can be determined from signal characteristics such as the frequency change with time, the final frequency, and the signal strength.

2.3 BINARY SYSTEMS COMPOSED OF A COMPACT STAR AND A MASSIVE BLACK HOLE

A potential source of information about massive black holes in galactic nuclei is gravitational radiation from compact stars tightly bound to them. If a neutron star, white dwarf, or 5–20 $M_\odot$ black hole in the density cusp around a massive black hole is deflected in close enough, it may become more tightly bound by gravitational radiation. However, if it is not fairly tightly bound to start with, it probably will be scattered by other stars and either drift away or come too close and plunge in directly. Other compact stars which are more tightly bound are

likely to be scattered less and have a good chance of losing a few percent of their energy by gravitational radiation over a period of perhaps 100 years before finally plunging in.

The number of compact star-MBH binary signals which may be observable by LISA and their signal strengths have been estimated [Sigurdson 1997; Hils and Bender 1995; Sigurdson and Rees 1997]. The results if the compact stars are neutron stars are shown in Fig. 2-2. Some of the assumptions made are as follows: 20% of all spiral and elliptical galaxies larger than 10^9 $M_\odot$ contain massive black holes; the massive black hole mass today is roughly 0.1% of the galaxy mass; 10% of the stars in the inner part of the cusp are compact; and the star density in the cusp can be scaled roughly from the results of Lauer et al. [1992] for M32. Most of the expected signals would come from red shifts of 0.1 or less and from massive black hole masses between roughly 10^6 and 10^7 $M_\odot$. It is interesting that the main limitation on detecting such signals might turn out to come from a confusion-limited background of extragalactic close white dwarf binaries (CWDBs), as discussed in the next section.

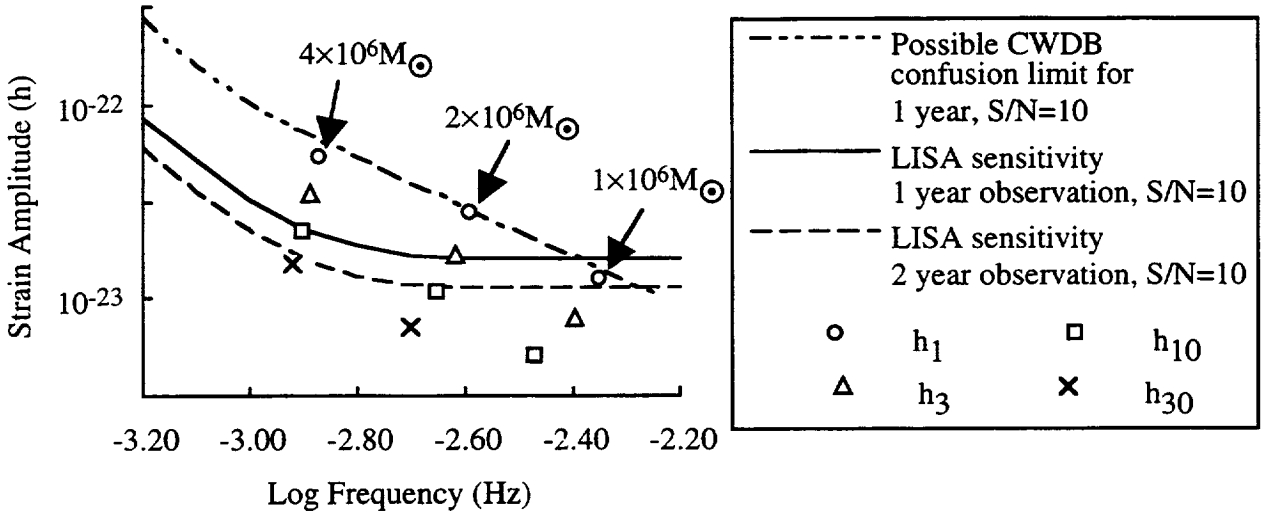

Figure 2-2 Strength of estimated compact star-massive black hole binary signals. Amplitudes h_j and frequencies f_j of the i-th strongest estimated sources for different massive black hole (MBH) masses. Different symbols are used for the strongest expected source for a given MBH mass, the 3rd strongest, the 10th strongest, and the 30th strongest. The solid and dot-dashed curves are the LISA sensitivity and a possible noise level due to close white dwarf binaries (see text) as in Fig. 2-1, but for an S/N of 10 instead of 5. The dashed curve corresponds to the sensitivity for a 2-year observation time, and the dot-dashed curve would be lowered by a similar amount in this case.

The orbits for compact star-MBH binaries start out being extremely elliptical, and remain quite elliptical [Cutler et al. 1994] until the angular momentum barrier is exceeded and the compact star plunges into the massive black hole. The compact star speed near periapsis is roughly a third of the speed of light, and the relativistic precession period for periapsis is similar to the radial period. If the orbit plane is tipped with respect to the equator of a rapidly rotating Kerr massive black hole, the precession of the orbit plane due to frame dragging will be quite fast. Thus, the gravitational wave signals from such binaries will be quite complex, and a signal-to-noise ratio of about 10 will be needed to identify them reliably.

The main astrophysical results obtainable from compact star-MBH binaries are a combination of information about conditions in the cusp around the massive black hole, the fraction of compact stars there, and the space density of massive black holes in the range of roughly 10^6 to 10^7 $M_\odot$ for which LISA is most likely to be able to detect the signals. In addition, even for a S/N of 10, the signals would permit tests of the predictions of general relativity for extremely high fields to a level which apparently is not achievable for any other proposed measurements. This is because the signals would be observed over roughly 3×10^4 cycles per year with periapsis distances of only a few Schwarzschild radii for the massive black hole. For example, Apostolatos et al. [1994] have shown that all of the moments of a black hole in a binary will be encoded in the gravitational waves. If the effects of these moments can be detected, it will be possible to verify whether all of the moments are indeed determined by just the mass and angular momentum of the black hole.

2.4 GALACTIC BINARIES

Another important objective of the LISA mission is to perform a detailed survey of gravitational wave signals from thousands of binary star systems in our galaxy [e.g. Hils, Bender, and Webbink 1990]. One type which may be observable is the neutron star (NS) [Narayan et al. 1991; Phinney 1991]. They would be observed at frequencies of roughly 1 to 3 mHz. The large majority of all observable galactic binaries will be near the galactic center. The upward sloping dashed straight line in Fig. 2-1 shows the signal strength vs. frequency for NS-NS binaries at the galactic center. The downward sloping dashed straight line gives the signal strength versus frequency for the closest NS-NS binaries.

There is a good chance that ground-based gravitational wave detectors will have detected a number of neutron-star coalescence signals at distances out to a few hundred parsecs (10^{15} km) before the LISA mission. That will determine the average number of short period NS-NS binaries in galaxies, as well as tight constraints on the equation of state for the neutron star matter. However, LISA would give information on how the space density of short period NS-NS binaries in our galaxy compares with that of average galaxies, which cannot be determined from pulsar observations.

The evolutionary scenario that is expected to lead to NS-NS binaries will also form neutron star–black hole (NS-BH) binaries in some cases. In fact, the formation of a black hole has much less probability of disrupting a binary system, since less mass is lost. For this reason, Narayan et al. [1991] estimated that there could be almost as many NS-BH binaries as there are NS-NS binaries. Tutukov and Yungelson [1986, 1993] considered this process in detail, and estimated that there should be about 10% as many NS-BH binaries as NS-NS binaries. It is possible that there also are a handful of binaries in the galaxy consisting of two 5–20 $M_\odot$ black holes which would be easily detected by LISA.

The short-dashed straight lines in Fig. 2-1 show the expected signal strength vs. frequency for close white dwarf binaries at the galactic center and for the nearest close white dwarf binaries on the assumption that the space density of close white dwarf binaries is 10% of that calculated by Webbink [1984]. With this assumption, the total number of close white dwarf binary signals from our galaxy is high enough below about 1 mHz that they cannot be resolved with 1 year of observation by LISA. The superposition of all these signals forms an apparent noise background, which a particular binary signal such as from a source near us would have to be above by about a factor 5 in order to be detected reliably. At higher frequencies there is a

lower but still important noise background due to the extremely large number of extragalactic close white dwarf binaries, with contributions from all galaxies out to large red shifts.

The sensitivity limit due to the assumed space density of close white dwarf binaries, both galactic and extragalactic, is shown by the dot-dashed curve in Fig. 2-1 At the lowest and highest ends of the frequency range, it is just 5 times the rms background signal in a 1 cycle/year frequency bin. In between, the curve is calculated using the probability that a given 1 cycle/year frequency bin will not have a typical strength galactic binary signal in it. It should be remembered that the sensitivity limit curve due to close white dwarf binaries is just a possible curve if the close white dwarf binaries have the assumed space density. The curve could be as much as a factor of 3 higher if the space density were a factor 10 above the assumed value, or it could be considerably lower. The location of the knee in the curve also would change with the space density. The corresponding sensitivity limit curve is shown in Fig. 2-2 also, but for an S/N of 10. For compact star–massive black hole binaries, the extragalactic close white dwarf confusion noise level could turn out to be the most serious limitation on the achievable overall sensitivity level.

In addition to the above types of binaries, it seems likely that signals from at least a few cataclysmic variables, contact binaries, and binaries consisting of unevolved stars will be mixed in with the other detected signals. *i Boo* and *WZ Sge* are known sources which may well be detectable, since their locations and frequencies are known, and thus an S/N of 5 is not needed to detect them reliably. Some nearby known interacting white dwarf binaries are likely to give strong gravitational wave signals at one of a few frequencies deduced from the optically observed signals. In addition, thousands of other interesting white dwarf binaries and their precursors are expected to be observable at frequencies below 3 mHz.

2.5 POSSIBLE COSMIC BACKGROUND

Some useful information also would be obtained by LISA concerning a possible cosmic background of gravitational waves. LISA could see a background level of 10^{-10} of the closure density near 1 mHz, or somewhat lower, depending on the close white dwarf binary background level. A pre-stellar level this high, based on relic gravitons from the Big Bang and standard inflation, would conflict with results for the microwave background isotropy from Cosmic Background Explorer (COBE). However, non-standard inflation models or other types of gravitational wave backgrounds generated by phase transitions or strings could give levels detectable by LISA near 1 mHz or ground-based detectors near 100 Hz without conflicting with the COBE results. In view of the uncertainty in generating mechanisms and the roughly 10^5 difference in sensitive frequencies, background observations by both LISA and ground-based detectors would be worthwhile.

SECTION 3—MISSION DESIGN

The three LISA spacecraft are to be launched on a single Delta-II 7925H. The initial orbit has an excess energy of $C_3 = 1.1\ km^2/s^2$ so that the three spacecraft will slowly drift behind the Earth. The desired final orbits have semimajor axis a = 1 AU (150×10^6 km), separation d = 5 million km, eccentricity $e = 2d/(a\sqrt{3})$, and inclinations $i = \pm 2d/a$. The spacecraft form an equilateral triangle with center in the ecliptic 20°(0.34 AU or 52×10^6 km) behind the Earth. After reaching the final orbits, the spacecraft evolve under gravitational forces only. Micronewton ion thrusters are used to keep the spacecraft centered about the shielded test masses within each spacecraft.

With this choice of orbit, the spacecraft separations remain fairly constant throughout the science operation period, nominally three years. Figure 3-1 shows how the formation evolves over the course of the year. Changes in the spacecraft separation are caused dominantly by the gravitational pull of the Earth. The changes in separation cause Doppler shifts of the laser signal. These Doppler shifts need to be removed by the interferometry electronics, with larger Doppler shifts being more difficult to deal with. The location of the center of the formation 20° behind the Earth represents a compromise between the desire to reduce the gravitational pull on the Earth and the desire to be closer to the Earth to reduce the amount of propellant needed and ease the requirements on the telecommunications system.

With the current orbits, the angle between the two distant spacecraft, as seen from any one spacecraft, changes slowly through the year, by ±1° in the worst case. This requires the angle between the two telescopes on each spacecraft to be articulated.

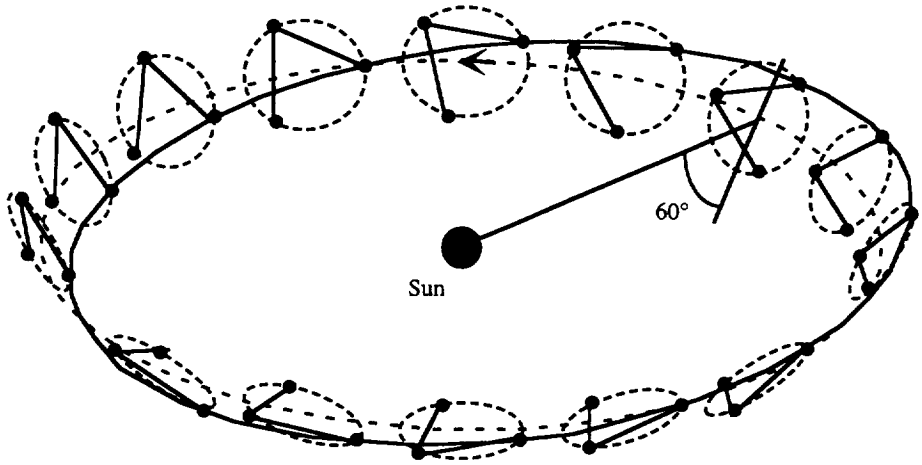

Figure 3-1 The orbits of each of the three LISA spacecraft inclined to the ecliptic by about 1° with an eccentricity about 0.01. The dashed line indicates the path of the center of the formation in the ecliptic plane while the solid line shows the orbit of one of the spacecraft. One of three possible interferometers is indicated by the lines between the spacecraft to show how it rotates as viewed from the formation center.

At launch, each spacecraft is attached to a propulsion module, with each spacecraft/propulsion module separating from each other after injection into the transfer orbit. The propulsion module provides the capability to maneuver the spacecraft into the final orbits. After reaching the final orbits, about 13 months after launch, the propulsion modules are

separated from the spacecraft to avoid having excess mass, propellant, moving parts, and/or solar panels near the test masses within the spacecraft. Two different propulsion technologies have been considered for placing the spacecraft into the operational configuration—chemical propulsion and solar-electric propulsion (SEP)—and two corresponding mission options were studied.

3.1 BALLISTIC CHEMICAL PROPULSION OPTION

Several individuals (E. Joe Cutting and Ted Sweetser of JPL and Friedhelm Hechler of the European Space Operations Center (ESOC)) have generated conic transfer trajectory solutions with impulsive maneuvers, all with slightly different strategies for the maneuvers and all taking about a year to place the spacecraft into operation. Hechler's trajectory, which required slightly higher launch energy (C_3 = 1.115 km^2/s^2) and slightly less post-launch ΔV (1050 m/s maximum per spacecraft, including 50 m/s for trajectory correction maneuvers) to do the transfer, was adopted as the initial baseline. The transfer takes 13 months. The maximum distance from the Sun during the transfer is less than 1.1 AU for all three spacecraft, and the distance from the Earth increases gradually to the distance in the operations orbit.

3.2 SOLAR-ELECTRIC PROPULSION OPTION

Carl Sauer (JPL) has generated a set of trajectory solutions, using low-thrust ion engines, which place the spacecraft in operations configuration in 400 days. The three trajectories require 19.1 kg, 13.9 kg, and 17.7 kg of xenon propellant respectively, assuming a 100% duty cycle and a 400-kg initial total mass. The ion engine considered was the Hughes XIPS thruster, which generates 18 mN of thrust and requires 500 W of electrical power. These trajectories were optimized for an assumed initial escape velocity vector and an assumed final operations configuration, but the parameters defining these assumptions (C_3, escape velocity direction, and operations triangle orientation angle) still need to be optimized. The launch energy used corresponds to a C_3 = 1.221 km^2/s^2. As with the chemical propulsion transfer above, the spacecraft drift gradually away from the Earth out to the operations orbit; none of them ever gets farther from the Sun than 1.07 AU (160×10^6 km) or closer than the operations orbit.

One important parameter for the SEP system is the thrust beam cone angle, which is the angle between the direction the ion engines are pointed and the Sun. This is important because if this cone angle stays close to 90° then the solar arrays and ion engines could be mounted with a fixed geometry. Unfortunately, the trajectory set found has this cone angle dropping below 35° for one of the spacecraft and below 50° for another; the cone angle never goes above 110° for any of the spacecraft. It is likely that varying the assumed operations triangle orientation angle will raise this minimum cone angle, but probably to a value near 40°; further improvement is expected for a lower launch energy but this could then force a longer transfer time if the C_3 is lowered below about 1.1 km^2/s^2. It may also be reasonable (in terms of increased propellant required) simply to impose a cone angle constraint, but current trajectory optimization tools do not include this capability.

The xenon propellant could probably be evened out by varying the assumed operations triangle orientation angle, but the maximum required would probably not decrease much. Also, we cannot predict what effect limiting the thrust beam cone angle might have. The maximum propellant required for this trajectory set, 19.1 kg, corresponds to a characteristic velocity (i.e., total ΔV) of 1241 m/s. We initially assumed for this study a propellant loading of 20 kg for each spacecraft for a ΔV capability of 1305 m/s. As the Team X study progressed, the injected

mass increased, so Propulsion ended up designing for 22 kg of propellant, which, considering the final mass and the need for residuals, probably corresponds to somewhat under 1300 m/s ΔV capability, but it is probably sufficient.

SECTION 4—SPACECRAFT DESIGN

The spacecraft design is based on a short structural cylinder 1.8 m in diameter and 0.48 m high. Figure 4-1 shows an artist's concept of the spacecraft design. The cylindrical structure supports a Y-shaped tubular structure, which serves as a thermal shield to reduce the effects of spacecraft power fluctuations or changes in the solar luminosity on the optical assemblies contained in two arms of the Y. The spacecraft equipment is to be mounted on the inside wall of the structural cylinder. Extending out from the structural cylinder is a Sun shield. In the operational orbits the Sun will be 30° from the normal to the top of the cylinder, and the Sun shield will keep sunlight off the cylinder wall. The main solar panels for the spacecraft are mounted on this Sun shield. A sheet of material across the top of the cylinder (not shown in Fig. 4-1) prevents sunlight from striking the Y-shaped payload thermal shield. The payload thermal shield is gold-coated and suspended by stressed-fiberglass bands from the spacecraft cylinder to thermally isolate it from the spacecraft. The optical assemblies in turn are thermally isolated from the payload thermal shield. The spacecraft cylinder and payload thermal shield are made of a graphite-epoxy composite chosen for its low coefficient of thermal expansion. Two 30-cm diameter X-band radio antennas (not shown) are to be mounted to the outside of the spacecraft for communication to the Earth.

Figure 4-1 Artist's concept of the LISA spacecraft. Not shown is a cover over the top of the cylinder that prevents sunlight from striking the Y-shaped payload enclosure.

Figure 4-2 shows the interior of the spacecraft and the layout for the payload. The two optical assemblies contain a 30-cm diameter telescope for transmitting and receiving laser light and an optical bench centered about a gold-platinum alloy test mass. The telescope and optical bench are mounted from a graphite-epoxy cylinder which is gold-coated to thermally isolate it from the payload thermal shield. The optical bench is supported from its support cylinder by low-thermal-conductivity rods. This, combined with the weak coupling of the support cylinder to the payload thermal shield and of the payload thermal shield to the spacecraft cylinder gives three stages of thermal isolation for the optical bench. The support cylinders for the two optical

assemblies are attached at the front to two actuators (not shown) and at the rear to a flexure mount. The flexure allows the optical assembly to be controlled in yaw and pitch by the actuators at the front. The pointing actuators allow a ±1° change in angle throughout the one-year orbit. The actuators are piezoelectric transducers mounted on a motor-driven worm screw. Aft of each optical bench is a disk (plate) that supports preamplifiers and electronics for the test-mass sensor and the interferometer photodetectors. Part of the light from each optical bench is reflected off the back of the test mass. This aft beam is steered by a mirror on the electronics plate to the other optical assembly for measuring the relative positions of the two test masses. The lasers for each optical assembly are mounted from an 80-cm diameter disk (not shown) attached to the bottom of the Y-shaped payload thermal shield. The laser light is transmitted to the optical bench through a single-mode polarization-preserving fiber.

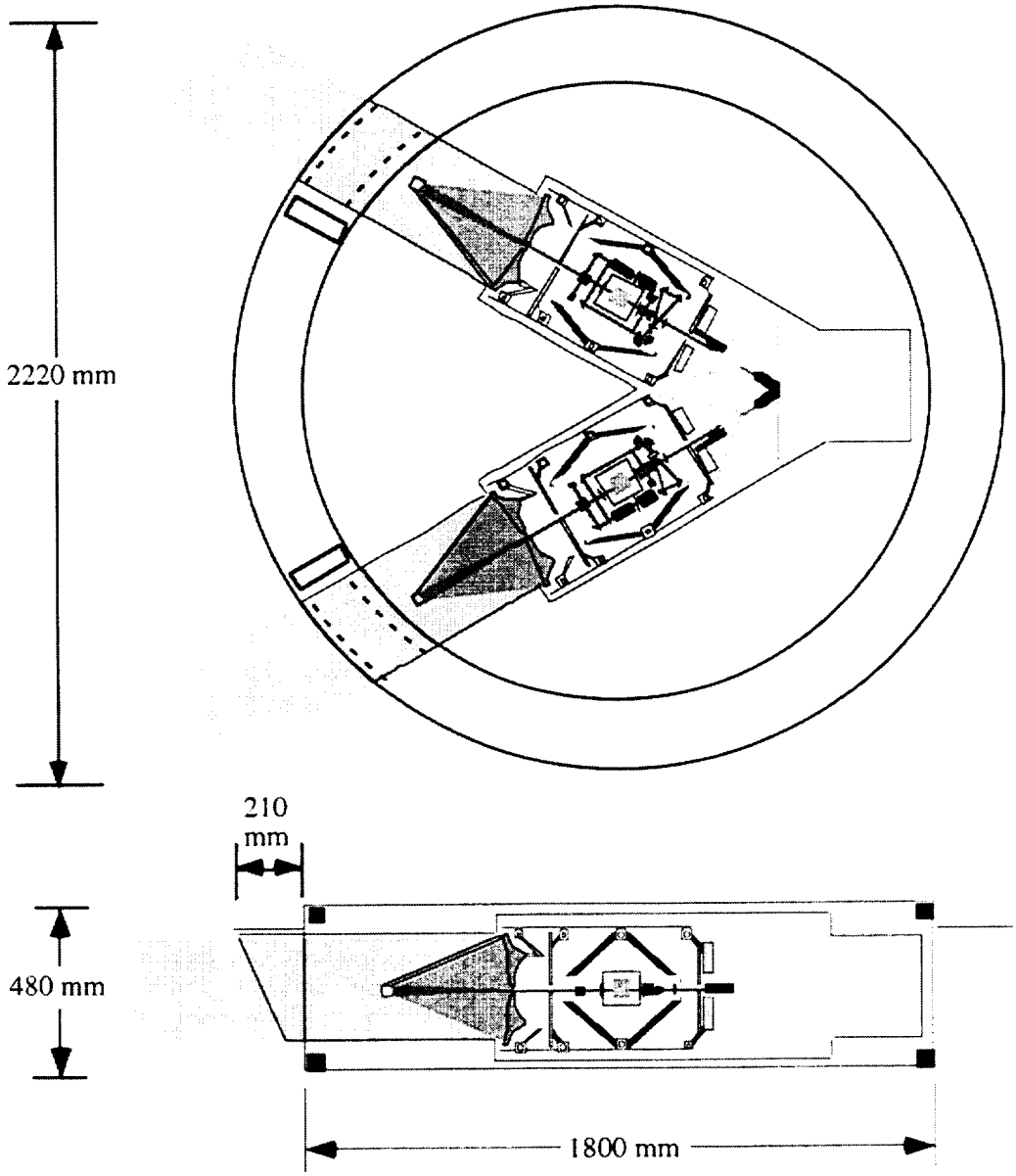

Figure 4-2 Top and side cross sections of the LISA spacecraft.

After launch the three spacecraft/propulsion module pairs separate from the launch vehicle and from each other. For the solar-electric propulsion option, two solar arrays are deployed after launch separation to provide the 500 W of electrical power needed for the ion engine. An artist's concept of the deployed configuration is shown in Figure 4-3. The extended solar panels are mounted on one-axis gimbals to track the Sun as the direction between the thrust axis and the direction to the Sun change throughout the 13-month cruise phase. The SEP stage contains two ion engines. Only one will be used at a time. The second engine is for redundancy and also balances the launch load. After reaching the desired science orbit, the propulsion module and deployed solar panels will be separated from the spacecraft.

The spacecraft size and shape are approximately optimized to contain the two optical assemblies within the payload thermal shield. This shape, combined with the desire to fit the three spacecraft with their propulsion modules within the Delta-II fairing, places volume constraints on the propulsion modules. Figure 4-4 shows the proposed launch configuration. The propulsion module is nominally contained within a cylinder 1.8 m in diameter and 0.4 m high. The launch configuration has a propulsion module on the top of the launch stack.

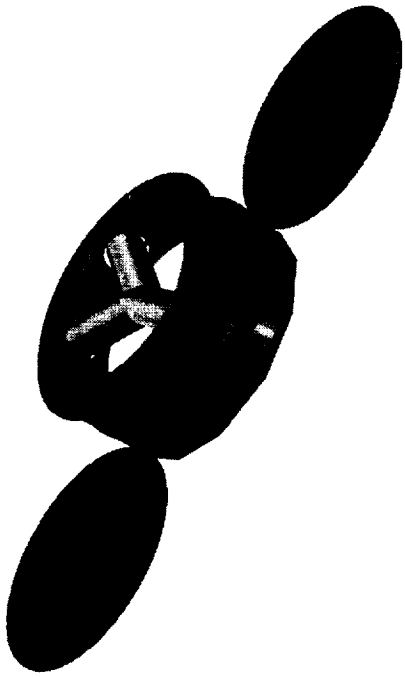

Figure 4-3 Artist's concept of the LISA spacecraft attached to the solar-electric propulsion module. The ion engine is mounted at an angle to the wall of the main cylinder of the propulsion module in order to thrust through the combined center of mass. The ion engine requires power from two deployable solar arrays which are gimbaled to allow for tracking the Sun. Not shown is a cover over the top of the cylinder that prevents sunlight from striking the Y-shaped payload enclosure.

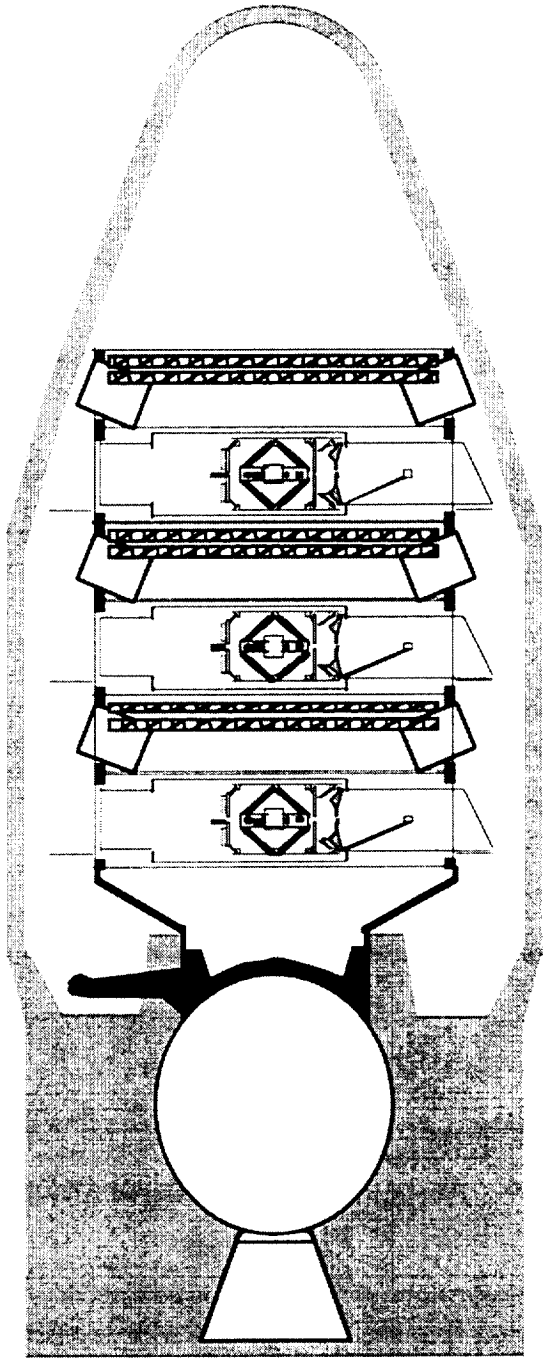

Figure 4-4 Launch configuration for the three LISA spacecraft, each with attached propulsion module, within the 2.9-m (9.5-foot) fairing for the Delta-II 7925H. The propulsion module indicated includes two xenon-ion thrusters with two deployable solar panels in the stowed position. The spacecraft assembly is attached to the upper stage by a custom launch adapter.

SECTION 5—SYSTEMS ENGINEERING

The mission was defined as three spacecraft to be launched on a common launch vehicle, preferably a Delta II. The science module, called here a "sciencecraft," together with a propulsion module constitute one spacecraft. After separation from the launch vehicle, the stacked spacecraft separate into three and are placed individually by their propulsion modules into a science orbit at 1 AU, trailing the Earth by 20°. Guidelines for the study were developed together with the science team and are given in Table 5-1. Mission duration was specified as a 13-month cruise to the science orbit followed by a 3-year science mission. Consumables were to be sized for an additional 7-year extended mission, for a total of 10 years of science, as long as this did not drive the design.

The sciencecraft attitude control subsystem controls the propulsion module and also provides coarse attitude control to the sciencecraft. Fine control is provided by the payload sensor using field-emission electric propulsion thrusters (FEEPs), which are provided as part of the payload. The FEEPs are the sole propulsion capability for the sciencecraft after the propulsion module is discarded.

Data return is at 7 kbps (bits/second) using an X-band (8 Ghz) link with two, 30-cm diameter, steerable (one axis) high-gain dish antennas and a 5-W transmitted power amplifier. Two antennas are required to provide coverage throughout the 1-year orbit. An emergency link is also provided.

For a 13-month cruise to final orbit and a 3-year science mission, the estimated radiation total ionizing dose is approximately 110 J/kg (11 krad). This estimate assumes 2.5 mm of aluminum or equivalent shielding and does not include a radiation design margin (RDM). An RDM of 2 should be considered for final parts selection.

Because of the mission duration and the requirement for three operating spacecraft, fully redundant spacecraft hardware was assumed.

A 30% mass and power contingency was applied to the instrument and the spacecraft (dry mass) to compensate for the early state of the design. It is expected that this contingency would be consumed during the development cycle, with the spacecraft launch mass and power growing to the numbers shown here.

The solar-electric propulsion module uses xenon-ion thrusters developed by Hughes for geosynchronous satellite station keeping. A deployed solar array is needed to provide additional power for the SEP system. This array is attached to the propulsion module and is discarded along with the rest of that module after reaching the science orbit. A 5% power contingency was applied for the SEP system since the maximum input power is well defined. A monopropellant attitude control provides for initial acquisition, roll control, and attitude control.

The systems summary sheet given in Table 5-2 gives breakdowns of mass and power requirements by subsystem. The summary shows a slightly negative mass margin. However the difference is sufficiently small that additional design work should produce comfortably positive margins on at least a Delta 7925H, and perhaps a lesser Delta II if further mass reductions can be found. It is recommended that at this stage of the design process the redundancy and

contingency mass approaches shown here be retained, and mass improvements be obtained through reductions in capability or higher technology hardware rather than by less conservative design or mass accounting.

Table 5-1 System design guidelines.

Guidelines	Programmatics/Mission
Customer	Pete Bender, University of Colorado
Study Lead	Richard Bennett
Mission	Gravity Wave detection
Target Body	Solar orbit at 150×10^6 km (1 AU), trailing Earth by 20 deg (52×10^6 km)
Trajectory	Science - 1 AU, slightly elliptical, slightly inclined
Science/Instruments	3 spacecraft, ea. with inertial sensor/test mass, 1-W laser ranging w/2 30-cm telescopes
Potential Inst-S/C Commonality	Instrument provides fine attitude sensing
Desired Launch Vehicle	Delta 7925H, 2.9-m (9.5-ft) shroud, despin performed by PAM-D
Launch Date	July 1, 2004
Mission Duration	13-mo. cruise; 3-year science required, 10-year goal (expendables)
Mission Class	Class B/C
Hardware Models	3 flt S/C + 1 (partial?) prototype/breadboard instrument

Guidelines	Spacecraft
Redundancy	Selected - high
Stabilization	3-axis
Heritage	None, custom
Launch Vehicle Capability	C3 = 1+, ~1400 kg
Radiation Total Dose	2.7 krad/year behind 0.025 mm (100 mils) Al, no RDM included; 11 krad baseline
Post-Launch Delta-V	~1350 m/s worst-case
Payload Mass	275 kg
Payload Power	150 W
Payload Data Rate	300 bps each spacecraft
Payload Pointing	None in cruise, science—provided by payload
Tracking Network	DSN, 34-m beam waveguide

Guidelines	Costing
Cost Target	$300 M (+ foreign supplied Test Mass, Laser, FEEPs)
FY$ (year)	1997
Phase A Start (month)	July
Phase A Start (year)	1999
Phase A Duration (months)	12
Phase B Duration (months)	18
Phase C/D Duration (months)	30
Phase E Duration (months)	49
Spares Approach	Selected
Parts Class	Commercial + Class B
S/C Supplier	Industry - custom
Instrument Supplier	Univ. Colorado + ESA
Integration and Test Site	S/C contractor
Launch Site	Eastern Test Range
Burdens—JPL Program Office	Space and Earth Science
Reserves	20%

Table 5-2 Systems summary for LISA using solar-electric propulsion.

	Mass (kg)	Mode 1 Power (W)	Mode 2 Power (W)	Mode 3 Power (W)		NASA TRL
Sciencecraft (ea.)		*Science xmit on*	*Propulsion Module -SEP*	*Launch*		
Payload						
Instruments	70.0	72.2	0.0	0.0		5
Thermal Tube	14.2	0.0				
Payload Total	84.2	72.2	0.0	0.0		
Bus						
Attitude Control	6.0	2.1	12.7	13.2		5
Command & Data	14.5	13.1	9.9	9.9		6
Power	12.2	14.8	6.8	9.5		
Structure	41.1	0.0	0.0	0.0		6
Cabling	15.1					
Propulsion (FEEPs incl. Drivers)	18.0	22.0	N/A	N/A		5
Telecomm	9.9	26.4	12.0	22.0		5
Thermal	1.7	0.0	17.0	17.0		7
Bus Total	118.6	78.4	58.4	71.6		
Sciencecraft Total (Dry)	202.8	150.6	58.4	71.6		
Mass/Power Contingency	60.8	45.2	17.5	21.5		
Sciencecraft with Contingency (ea.)	**263.6**	**195.7**	**76.0**	**118.5**		
				Incl. PM		
Propulsion Module (ea.)						
Structure/Mechanisms	52.0	N/A				6
Thermal	3.0	N/A	17.0	17.0		7
Propulsion - SEP	44.2	N/A	490.0	0.0		6
Propulsion - Hydrazine	7.6		0.8	0.0		7
Power	12.6	N/A	26.9	0.0		
Solar Array Actuators/Electronics	4.2		1.0	2.5		7
Cabling	8.0	N/A				
Prop Module Total (Dry)	131.6	N/A	535.7	19.5		
Mass/Power Contingency	39.5	N/A	37.9	5.9		
Dry Prop Module w/Contingency	**171.1**	**N/A**	**573.6**	**25.4**		
Propellant & Pressurant - SEP	22.0	Propellant based				
Propellant & Pressurant - Hydrazine	4.8	on S/C mass =455				
Wet Prop Module with/Contingency (ea.)	197.9					
Total for 3 Sciencecraft/Prop Module	**1384.4**					
S/C Adapter	20.9	w/30% contingency				
L/V Adapter *Delta supplies*	0.0	w/10% contingency				
Launch Mass	**1405.3**					
Launch Vehicle Capability	1388.2	Delta 7925-H		1.221	Launch C3	9
Launch Vehicle Margin	**-17.2**		**-1.2%**			

Contingencies		
	Mass	Power
Instruments	30%	30%
Other	N/A	N/A
S/C, dry	30%	30%

except SEP power

Stabilization: cruise	**3-axis**	Pointing Direction: cruise	**Sun**
Stabilization: science	**3-axis**	Pointing Direction: science	**Inertial**
Radiation Total Dose, krad	**11 krad**	Mission Duration	**4.1 years**
Bit Error Rate	1.00E-05	Instrument Data Rate	**200 bps**
Redundancy	**High**	Data Storage	**3 Mbytes**

SECTION 6—INSTRUMENT

6.1 INSTRUMENT DESCRIPTION

The payload for each spacecraft consists of two optical assemblies, a surrounding structure, and lasers mounted on a disk-shaped radiator. Figure 6-1 shows a cross section of the two optical assemblies. Each optical assembly contains an f/1 Cassegrain telescope. The primary mirror is a double-arch lightweight ultralow expansion (ULE) design. The secondary is supported by a three-leg graphite-epoxy spider. The final quality of the plane wavefront leaving the telescope is $\lambda/30$. Each optical assembly also has an optical bench, machined from a block of ULE glass with dimensions $20 \times 35 \times 4$ cm, which contains injection, detection, and beam-shaping optics. A drag-free sensor (or "accelerometer") is mounted to the center of each optical bench. The test mass of the drag-free sensor acts as the mirror at the end of the interferometer arm.

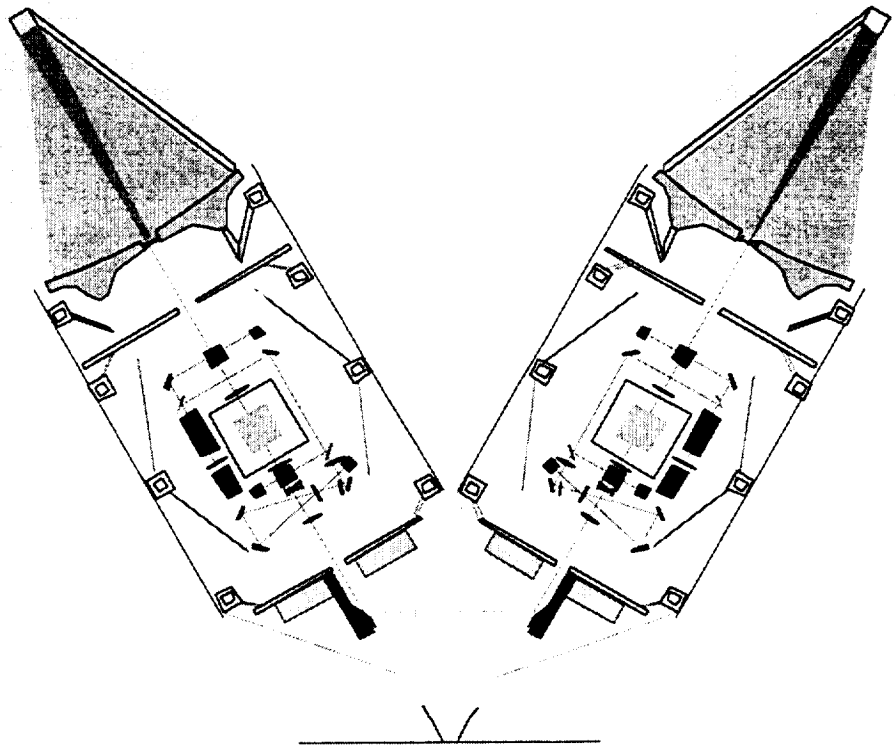

Figure 6-1 Cross section of the two optical assemblies comprising the main part of the payload on each LISA spacecraft. The two assemblies are mounted from flexures at the back (bottom of figure) and from pointing actuators (not shown) at the front, near the primary mirrors.

The laser beam is carried to the optical bench within each optical assembly by an optical fiber. About 1 mW is split off the 1-W main beam to serve as the local reference for the heterodyne measurement of the phase of the incoming beam from the far spacecraft. Also, about 1 mW is split off and directed towards a triangular cavity which is used as a frequency reference. The incoming light from the telescope is reflected off the test mass and superimposed with the local

laser on the phase-measuring diode. A small fraction (a few mW) of the laser light is reflected off the back of the test mass and sent for phase-comparison with the other optical assembly via a steerable aft-mirror. The aft mirror is controlled using the signal from an auxiliary quadrant photodiode, which senses the direction of the incoming beam from the other central spacecraft. By bouncing the laser beams off the test mass in the manner described, the interferometric measurement of test mass position is, to first order, unaffected by motion of the surrounding spacecraft.

A thin graphite-epoxy disk is mounted between the telescope and the optical bench to thermally isolate the bench from the telescope. The telescope will have an equilibrium temperature near 220 K while the low-expansion properties of the ULE optical bench are optimized for near room temperature. Behind the optical bench is a graphite-epoxy disk with the accelerometer preamplifiers, the diode preamplifiers, and an ultrastable oscillator (USO) mounted on it. All other electronics will be outside the payload cylinder.

The laser consists of two monolithic ring YAG (yittrium-aluminum-garnet) crystals in series, each pumped by two laser diodes. The nominal single-mode output power is 2 W at a wavelength of 1064 nm. For the LISA this was been downrated to 1 W to improve lifetime and aging properties. The operating temperature for the diodes and the YAG-crystal will be maintained by heaters. A complete spare laser will be carried for each optical assembly. The lasers are mounted on a carbon-carbon disk designed to radiate away the heat generated by the laser. This radiator disk, 80 cm in diameter, is mounted at the bottom of the payload thermal shield.

The drag-free position sensor is derived from the electrostatic accelerometer developed by the Office Nationale d'Etudes et de Recherches Aerospatiales (France). It contains a 4-cm cubic test mass made of a gold-platinum alloy with magnetic susceptibility less than 10^{-6}. This test mass is freely floating inside a gold-coated ULE cage, which supports the electrodes for capacitive sensing of attitude and position. The ULE-box is enclosed in a vacuum-tight titanium housing connected to the outside of the spacecraft by a tube to keep the interior of the accelerometer at a pressure of less than 10^{-6} Pa (10^{-8} mbar). Electrostatic charging of the test mass due to cosmic ray protons with energies in excess of 100 MeV would cause noise on the test mass as it moves through the solar magnetic field. Active discharging is achieved by directing ultraviolet light from a mercury discharge lamp at the test mass and walls, similar to the approach proposed for Gravity Probe B.

In the frequency range above 10^{-3} Hz, the LISA displacement noise level is below 20 pm/$\sqrt{\text{Hz}}$. Below 10^{-3} Hz, down to 10^{-4} Hz, performance is limited by spurious accelerations. These consist partly of real accelerations (such as residual gas impacts on the test masses) and partly of several thermal distortion effects that acquire an approximately $1/f^2$ dependence in displacement (the leftmost sloping curve on the LISA sensitivity plot in Fig. 2-1). The displacement error is dominated by photon shot noise (the floor of the sensitivity plot in Fig. 2-1).

One laser on one spacecraft will serve as the master and will be locked to the onboard reference cavity. The lasers on the other optical assembly, and on the other spacecraft, will be phase-locked to the master laser via the phase comparison beam exchanged between the incoming beams and the local laser.

A thermal model of the spacecraft suggests a temperature stability of the optical bench of about $1\mu K/\sqrt{Hz}$ at 1 mHz [Folkner et al. 1994]. With an expansion coefficient of $3\times10^{-8}/K$ for ULE, this leads to a frequency noise of $10\ Hz/\sqrt{Hz}$ for the laser. Because the arm lengths are unequal due to perturbations on the orbits, a laser phase noise correction scheme will be used that deduces the laser frequency fluctuations from the sum signal of the two interferometer arms and then subtracts their effects out from the signal [Giampierri et al. 1996]. For this technique, the arm length and the arm length difference need to be determined absolutely to about 1 km and 20 m, respectively. This is achieved by X-band radio tracking from the ground combined with laser phase information.

Due to the solar system disturbances, the spacecraft will have a small but varying velocity relative to each other, causing a Doppler-shift of the returning beam on the order of 5 MHz. The signal cannot be telemetered to the ground at that rate since the science data rate is limited to about 100 bps. Instead, a local USO is used to heterodyne the signal down to audio frequencies.

Initial beam acquisition will rely on star trackers to align the spacecraft to better than 10^{-4} rad. The laser beam will then be de-focused from its diffraction-limited divergence and imaged in the receiving spacecraft on quadrant diodes and charged-couple devices (CCD) arrays. Their signal will be used to iteratively re-point the spacecraft until the laser beam divergence can be reduced to the minimum value. Operational attitude control signals will be provided by the main signal detection diodes, the difference between the signals from their quadrants giving information on wave-front tilt. The pointing jitter is expected to be less than a few $nrad/\sqrt{Hz}$ which, for an outgoing wave front deformation of less than $\lambda/30$, leads to an apparent displacement noise less than the design goal.

The laser phase data will be processed on board the spacecraft for compression to 1-second average phase readings, which will be telemetered to the ground. X-band communication will be done with 30-cm diameter antennas to the Deep Space Network 34-m antennas with one 10.5-hour tracking pass on alternate days. Ground data processing to recover the gravitational wave signals will involve standard spectral and matched filter analysis once the frequency noise has been removed by correlating the signals from the two arms. The spectral resolution from 1 year of observations (3×10^{-8} Hz) coupled with a desired signal-to-noise ratio of 5, led to the sensitivity curve in Fig. 2-1.

6.2 INSTRUMENT DEFINITION

The mass breakdown of one optical assembly is given in Table 6-1. Table 6-2 gives the mass breakdown for the payload thermal shield, and Table 6-3 lists the masses of the lasers and the associated radiator. The payload mass excluding the 14-kg thermal shield is 70 kg. The power requirements for each optical assembly are given in Table 6-4, with 72 W total needed for the instrument.

6.3 INSTRUMENT COST

The instrument cost estimate was initially developed from the Aerospace mass model. Input mass to the model excluded both structure and payload thermal as not being instrument cost drivers. It was then estimated that one-fourth of first unit cost was non-recurring and the other three-quarters recurring. For the two subsequent units, it was estimated that one-tenth of the first unit assigned "non-recurring" cost would actually attach to each further unit and that the

"recurring" effort would decline to two-thirds of its first unit value. The cost breakdown derived is given in Table 6-5.

Table 6-1 Mass breakdown for optical assembly.

Item	Mass (kg)	Description
cylinder	2.85	3-mm wall, 36-cm diameter, 50 cm long
stiffeners	0.48	2-mm wall, 1-cm diameter, 36 cm around, 4 ea
mirror	3.83	
mirror support	2.00	
secondary	0.50	
secondary support	0.50	
bench supports	0.30	
electronics plate	0.59	5 mm thick, 30-cm diameter
plate supports	0.10	
thermal shield	0.12	1 mm thick, 30-cm diameter
shield supports	0.10	
accelerometer	5.00	
bench	4.10	20x35x4 cm, minus 6x6x4 cm, ULE, less 30% for machining
pointing device	1.00	Newport precision actuator
accelerometer electronics	2.00	
laser electronics	1.80	analog-to-digital (A/D) converter, diodes, laser control
USO	1.30	Mars Observer
payload power regulator	1.00	
Mercury lamp	1.00	Gravity Probe B
Total	**28.57**	

Table 6-2 Mass breakdown for lasers and radiator.

Item	Mass (kg)	Description
radiator	4.22	80-cm diameter, 5 mm thick
lasers	8.60	Laser Zentrum lasers, 4 ea
Total	**12.82**	

Table 6-3 Mass breakdown for payload thermal shield.

Item	Mass (kg)	Description
front tubes	3.99	2-mm wall, 32-cm diameter, 59 cm long, 2 ea
front stiffeners	0.21	1-mm wall, 1-cm diameter, 32 cm around, 4 ea
middle tubes	4.48	2-mm wall, 40-cm diameter, 53 cm long, 2 ea
middle stiffeners	0.53	2-mm wall, 1-cm diameter, 40 cm around, 4 ea
transition	2.96	2-mm wall, 40-cm diameter, 70 cm long, 2 ea
aft tube	0.78	2-mm wall, 32-cm diameter, 23 cm long
aft stiffeners	0.11	1-mm wall, 1-cm diameter, 32 cm around, 2 ea
aft plate	0.14	1 mm thick, 32-cm diameter
flexure support	1.00	
Total	**14.19**	

Table 6-4 Optical assembly power requirements.

Item		Power (W)
Laser		18.0
Diode lasers	8.0	
Diode heaters	8.0	
Laser crystals	1.2	
Laser heaters	0.8	
Laser temperature preamps		0.3
Laser and servo electronics		2.4
Accelerometer electronics		4.0
Photodiodes		0.1
Photodiode preamps		0.3
Phase modulator		0.1
Aft mirror		0.5
Payload power regulator		1.5
A/D converter		1.0
USO		3.0
NPO (numerically programmed oscillator)		1.0
Phase modulator electronics		0.4
USO		1.3
Payload power unit		1.0
Pointing actuators		0.1
Mercury lamp		1.0
Total		**36.0**

Table 6-5 Estimated instrument cost (for first spacecraft).

Subsystem	Cost ($M)
Design	8.9
Test hardware	2.1
Testing	3.8
Flight hardware	18.5

SECTION 7—PROPULSION

7.1 SOLAR-ELECTRIC PROPULSION

LISA requires a propulsion module for the velocity increments to transfer to, and to insert into, the final mission orbit. As long as the propulsion module is attached to the spacecraft, it also provides the reaction-control torques required.

The solar-electric propulsion (SEP) system uses an ion engine for main propulsion functions, together with a monopropellant hydrazine (N_2H_4) system for attitude control. The SEP system was based on the Hughes XIPS thruster to be flown on the Galaxy IIIR Communications Satellite. All components of both the SEP and the N_2H_4 systems exist, except the tank for the SEP system would be a new development to fit the propellant capacity required for that system. Some of the characteristics of the ion thruster are given in Table 7-1.

Two thrusters are assumed for this system to provide redundancy. One power processing unit (PPU) is used for each thruster. The propellant requirement for this system is determined by Mission Design for the trajectory flown. The Xe propellant requirement was determined to be 22 kg. The mass of the SEP subsystem is given in Table 7-2.

The N_2H_4 Attitude Control Propulsion System was assumed to be a simple blowdown system with one tank and eight thrusters. The thrusters were assumed to be a complement of four 4.45-N, and four 0.9-N thrusters. In this application, the thrust would reduce over a 3:1 ratio during the mission as the non-regulated tank pressure blows down. An existing tank from Pressure Systems Inc. (model 80216-1) is applicable for the approximately 5-kg propellant requirement assumed. The tank has a 6Al-4V titanium shell and an elastomeric AF-E-332 positive-expulsion diaphragm. The mass estimate for this subsystem is given in Table 7-3.

Total cost for the propulsion system combination is estimated to be $24.9M for three propulsion modules. The cost breakdown is as follows:

Design, analysis, procurement engineering, and management:
- $1.55M SEP 1st system; $0.52M each for 2nd & 3rd systems
- $1.55M N_2H_4 1st system; $0.52M each for 2nd & 3rd systems

Fabrication, assembly, system test, and subsystem ATLO support:
- $1.14M SEP 1st system; $1.03M each for 2nd & 3rd systems
- $1.14M N_2H_4 1st system; $1.03M each for 2nd & 3rd systems

Procurements:
- $4.06M SEP 1st system, including spares for all systems
- $2.73M each for 2nd & 3rd systems
- $1.31M N_2H_4 1st system (no spares)
- $1.25M each for 2nd & 3rd systems

Table 7-1 Characteristics of the SEP thruster.

Thruster Size	~22-cm diameter ~25-cm height
Thruster Power	440 W
Thrust at full power	17.8 mN
Specific impulse at full power	2585 s
Service life	6000 h tested to date 18000-h goal

Table 7-2 SEP system mass.

Element	Mass
Thrusters (2)	12.0
PPU (2)	13.6
Digital control interface unit (1)	2.0
Cabling, estimate	1.0
PPU thermal	3.2
Thruster gimbals	4.4
Feed system components	4.3
Tank (composite, overwrapped)	3.7
Xe propellant	22.0
Total loaded mass	66.2

Table 7-3 Hydrazine system mass.

Element	Mass
Thrusters (8)	2.3
Feed system components	4.0
Tank	1.3
Hydrazine propellant	4.7
Nitrogen gas pressurant	0.1
Total loaded system	12.4

7.2 FEEP PROPULSION

Once reaching the operational orbit, the propulsion module is separated from the spacecraft. Attitude and position control of the spacecraft are then performed by small ion thrusters. The field-emission electric propulsion (FEEP) thrusters are being developed at Centrospazio, with support from ESA. Six clusters, each containing four thrusters, would be mounted on the outside of the main structural cylinder of each spacecraft. This arrangement was chosen to provide full control in the case of the loss of one thruster or one cluster of thrusters. The specifications for each thruster are 1 to 100 μN thrust, with a noise level of 0.1 μN or less. The FEEP thrusters can be operated in either a continuous mode or a roughly 50% duty cycle modulated mode.

The mass and power for the FEEP system assumed for the study are given in Table 7-4. The FEEP subsystem was assumed to be provided by ESA and was assumed to cost $10M, based on preliminary numbers from an earlier ESA study

Table 7-4 FEEP system mass and power.

Element	Mass (kg)	Power (W)
Thrusters (24)	6	-
Control units (6)	12	22

SECTION 8—STRUCTURES

The basic structural configuration for each module has an exterior cylinder with a top and bottom plate to stiffen the cylinder and provide mounting points for the subsystems. The solar array is mounted to the sciencecraft's top plate/sunshield. To minimize the effects of thermally induced changes, all structural components must be composite materials with stiffeners (tubes or rings). The initial concept has each pair of modules connected with a circumferential clamp band that spans two interface rings, each of which is connected to its exterior cylinder. The stack of six modules with their conical adapter to the launch vehicle has been analyzed, and they meet or exceed the Delta launch vehicle requirements on lateral frequency >15 Hz, and axial frequency >35 Hz.

The two high-gain antennas are 30-cm diameter dishes, actuated (gently!) single-axis 7° once each week (2 minutes motion time), with a 180° total motion range. They will be mounted at the edge of the ring to look past the rim of the solar array/heat shield; they may require a fold-out structure to position them after separation.

Each propulsion module carries two separation systems, so that the sciencecraft will not be burdened with them. The mass of the separation system needs to be better defined in future work, due to the science team's choice to drop the clamp-band separation system in favor of explosive bolts, given the large mass of the clamp-band system.

8.1 SCIENCECRAFT STRUCTURE

A short general comment to the mass tables: Primary structure supports the Attitude Determination and Control System (ADCS), Command and Data System (CDS), telecom, bus-mounted power electronics and batteries, dry propulsion system, thermal blankets and heaters, and instruments. Secondary structure allows for junctions, stiffeners, brackets and fittings, solar array/antenna and other outrigger support (if any), and strengthening for liquid propellant mass. Interface and integration hardware covers fasteners, shims, and such. Balance mass is normally bookkept at 1% of spacecraft dry mass for a three-axis stabilized vehicle and 2.5% if the vehicle is spin-stabilized or is launched on a spinning upper stage. The adapters are scaled to the (wet) spacecraft launch mass. If the launch vehicle is identified and adapter data is available, that value will be used for the launch-vehicle side adapter.

In addition to the cabling required to interconnect the sciencecraft subsystems, there is also a need for additional pass-through cabling, connectors, and wiring separation devices for as many as (in the case of the "bottom" module) five separate stacked modules. This had not been considered when the original mass table (Table 8-1) was generated, so that the realistic cabling mass may well exceed the cabling estimate cited below.

In the present study, the specific structure configuration developed by the science team was used in generating the mass estimates. The secondary structure category, as well as the balance mass, were reduced to the values shown at the direction of the science team, presuming special care in design and component selection. The science team based this on a detailed study of the ESA design, which found 0.5% balance mass needed due to the symmetry of the spacecraft design. JPL's long project experience indicates that such optimism may not materialize in the face of actual flight hardware.

Table 8-1 Sciencecraft structure mass.

	Units	Mass, total (kg)
Primary Structure		32.0
Secondary Structure		2.5
Antenna Articulation Mech. (1-axis)	2	2.4
Interface and Integration Hardware		3.2
Balance Mass	(spinner)	1.0
Adapter, Spacecraft side		16.1
Cabling		15.1
Total		**72.3**

Table 8-2 Sciencecraft structure cost ($M).

	Total	Non-R.	Recurr.	Design	Dev. Test	Qual. Test	Flt. H/W
Bus Structure	4.50	2.50	2.00	2.30	0.20	0.20	1.80
Prop. Module (costed separately)	0.00	0.00	0.00				
Antenna Articulation Mech. (2)	1.50	0.70	0.80	0.60	0.10	0.10	0.70
Integration Hardware & AHSE	0.50	0.30	0.20	0.20	0.10		0.20
Misc.	0.60	0.30	0.30	0.20	0.10	0.05	0.25
Adapter, Spacecraft side	0.30	0.20	0.10	0.20			0.10
Cabling	0.70	0.40	0.30	0.40		0.05	0.25
Total	8.10	4.40	3.70	3.90	0.50	0.40	3.30

8.2 PROPULSION MODULE STRUCTURE

To supply the power needed by the SEP system, the propulsion module for the SEP has two double-panel solar arrays that fold out from the base of the 1.8-m diameter propulsion module around the edge of the separation ring. If we allow 2-cm stacked thickness for each panel, that gives 8-cm total, leaving 32-cm net thickness for the propulsion components.

A single-axis actuator is needed for each deployed solar array, with about a 70° range without bumping into the bus structure, so the whole thing needs to deploy out away from the separation ring. The solar array mass is bookkept under Power and the solar array actuator under ADCS, but the solar array structure and the launch latch/release hardware are bookkept here under Structures.

There is concern about mounting the 22 x 25-cm thrusters at about 70° from the centerline (pointed through the spacecraft/propulsion module combined center of mass) to fit into the 32-cm available height without fouling the separation rings (sticking out through a hole in the exterior cylinder—possible strength/stiffness concern).

To further complicate the design, the thrusters need a gimbal system to give about 5° adjustment. This has to be mounted to the back end of the thruster body due to space constraints (note that the gimbal system must maintain the thrust vector through the center of mass).

To avoid the high mass of the clamp-band system, the team wanted to consider a six-bolt pyro interface between the modules, thus changing the structural interface from the continuous clamp band to discrete hard points. Without any specific design layout or analysis, it was presumed that the mass based on the previous exterior cylinder plus the two clamp rings would be sufficient if re-allocated for the strut bipod structures to the pyro bolt interface points. It was also assumed that there would be less mass than for the chemical option in the top and bottom plates, and that, anyway, there could be no bottom plate because of the solar arrays, at most a stiffening flange. Nevertheless, structure is needed to mount the 21×42-cm xenon tank and 24-cm diameter hydrazine tanks, as well as the two engines, the power electronics modules, and the solar array mounts.

The structure also has to support the carry-through loads imposed by the (up to five) modules mounted above, and there would be concern whether the discrete interface points and the associated structure would have the rigidity necessary to meet the Delta's natural frequency requirements. This change in the structural concept would, of course, also apply to the sciencecraft module, with possible impacts on the telescope mountings. The Team-X structures representative can only caution that substituting the discrete interface concept with pyro bolts for the original continuous clamp band interface may not bring the hoped-for mass savings after all the affiliated engineering problems have been addressed.

Table 8-3 Solar-electric propulsion module structure mass.

Element	Mass (kg)
Outer cylinder, 40 cm high, 1.8-m diameter, 2-mm wall	7.5
Interior structure	8.
Interface Rings (2)	11.
Joints, fittings	4.
Separation pyro bolts	2.5
Solar array structure, hinges	12.
Solar array release mechanism (2)	3.
Interface hardware & misc.	3.
Balance mass	1.
Cabling	8.
Total (less launch vehicle adapters)	60.

Table 8-4 Propulsion module structure cost ($M).

	Total	Non-R.	Recurr.	Design	Dev. Test	Qual. Test	Flt. H/W
Bus Structure	3.70	2.00	1.70	1.90	0.10	0.10	1.60
Solar Array Structure	0.60	0.30	0.30	0.30			0.30
Solar Array Release Mech. (2))	1.30	0.60	0.70	0.50	0.10		0.60
Separation Mech.	1.40	0.40	1.00	0.30	0.10	0.10	0.90
Antenna Articulation Mech. (2)	1.50	0.70	0.80	0.60	0.10	0.10	0.70
Integration Hardware & AHSE	0.50	0.30	0.20	0.20	0.10		0.20
Misc.	0.60	0.30	0.30	0.20	0.10	0.05	0.25
Adapter, Spacecraft side	0.30	0.20	0.10	0.20			0.10
Cabling	0.70	0.40	0.30	0.40		0.05	0.25
Total	10.60	5.20	5.40	4.60	0.60	0.50	4.90

SECTION 9—ATTITUDE DETERMINATION AND CONTROL SYSTEM

9.1 INTERFACES

During normal on-orbit operation of the three LISA spacecraft, if all three arms of the interferometer are in use, the sensor signals for control of the spacecraft position and orientation will all come from the payload. However, star trackers will be needed for initial orientation of the spacecraft so that laser-beam signals can be acquired, and possibly for control of roll for one or two of the spacecraft if some of the optical direction sensors are not functional.

The main attitude control information from the payload will come from observations of the laser beams sent from the other two spacecraft. In its simplest form, the direction measurement system would operate as follows. After each 30-cm diameter telescope condenses the received beam down to 3 mm in diameter, about 10% of the received light is redirected by a beam-splitter and a 1-m effective focal length optical element to a quadrant detector. The differences of the outputs from the four quadrants give the angular position of the distant spacecraft with respect to the optical axis defined by the optical system and the position of the quadrant detector. Different audio frequency modulations of the transmitted beams are used to discriminate against scattered light from the same spacecraft.

The relative position control information from the payload will be generated by the two inertial test-mass sensor units (so called drag-free accelerometers) located 540 mm apart on opposite sides of the spacecraft center of mass. Each unit contains a freely floating cubical test mass and seven pairs of capacitive plate sensors for determining the position and orientation of the test mass within its housing.

The position and pointing readouts are provided by analog inputs; we assume that they will be digitized with 12-bit sampling by an A/D board in the payload central processing unit (CPU). The number of inputs is nominally three position and three translation for each test mass and two pointing for each telescope, a total of 16 inputs. An algorithm provided by the instrument/payload CPU will produce three position and three angular digital outputs for use by the Attitude Determination and Control System (ADCS) in developing spacecraft commands to control six degrees of freedom for an array of 24 field-emission electric propulsion (FEEP) micronewton thrusters

For the interface from the ADCS computer to the FEEPs, we assume that the FEEP power control units (PCU) will accept a 12-bit digital input for each thruster (24 total inputs) to control the thrust.

9.2 GENERAL REQUIREMENTS

Each of the three spacecraft shall have identical ADCS designs. Each spacecraft will be three-axis stabilized. All pointing control will be provided by either the hydrazine or FEEP thrusters systems.

Each of two high-gain antennas (HGA) will be articulated in one axis. The pointing requirement for the HGAs will be ±0.25°. The normal vector of the body mounted solar arrays shall be

pointed to within ±30° of Sun line during all phases of the mission with the exception of planned orbit change maneuvers, trajectory correction maneuvers (TCM), and HGA communication with Earth.

HGA actuators will be provided by the Structures subsystem. HGA drive electronics, control algorithms, and software will be provided by the ADCS.

Multiple, coarse silicon diode Sun-presence sensors will provide 4π-steradian coverage to acquire the Sun at any attitude in case of any loss of pointing control and/or knowledge.

Dual-redundant sets or internally redundant ADCS hardware will be required to meet the mission reliability requirements and goals.

9.3 OPERATING MODES

9.3.1 Launch and cruise mode

Pointing control requirements will be based on the solar arrays, high-gain antenna, and main-engine firings. During any maneuvers, the thrust-vector pointing control requirement will be within ±1°. Pointing knowledge will always be less than the control requirement, and if not driven by any other requirements, pointing knowledge will be 10% to 50% of the control requirements. There are no pointing stability requirements.

After launch, the three spacecraft and PAM-D upper stage in their stacked configuration will be despun by a yo-yo mechanism from 60 rpm to 0 rpm. The propulsion systems of the three spacecraft and their propulsion modules will not be used for despinning; however, extra fuel could be budgeted to back-up the yo-yo system.

All attitude control will be provided by the eight 0.9-N hydrazine thrusters during cruise. Four 0.9-N thrusters will provide roll control for the spacecraft. The other four 0.9 N thrusters will also provide pitch and yaw control, and most importantly, ensure a safe separation maneuver for the three spacecraft after burnout of the solid motor upper stage.

Angular rate information will be supplied by an inertial reference unit (IRU) during launch, launch vehicle separation, and throughout the cruise phase. Multi-star tracking with at least one star camera will be required to provide three axes of absolute attitude reference during cruise.

9.3.2 Separation from propulsion module

After separation of the propulsion module, FEEP micronewton thrusters will be used for attitude and position control. Six clusters, each containing four thrusters, would be mounted on each spacecraft. The specifications for each thruster are 1 to 100 μN thrust, with a noise level of 0.1 μN or less at periods of 1, 10, 100, 1000, and 10,000 s. The FEEP thrusters can be operated in either a continuous mode or a roughly 50% duty cycle modulated mode.

Initial estimates provided by the science team is that a ΔV of 3 cm/s will be given to the spacecraft after mechanical separation between the spacecraft and propulsion module. This ΔV was based on the numbers used for the Galileo probe separation mechanism. Table 9-1 shows estimates for the time it will take the FEEP thrusters to counteract the impulse generated by the

separation mechanism to the spacecraft. The estimates for 3 cm/s are highlighted in boldface. These estimates are based on a 250-kg spacecraft and 100-μN FEEP thrusters.

Careful consideration must be taken to ensure that no debris during separation will obstruct the views of the ADCS sensors (star cameras, sun sensors). Obstruction of one of Mars Pathfinder's Sun sensors has rendered that sensor unusable.

Table 9-1 Time in minutes for countering separation mechanism impulse.

	Number of FEEP Thrusters Fired		
Δv (m/s)	1	2	3
0.01	3.7	2.6	1.9
0.03*	**6.5**	**4.6**	**3.2**
0.10	11.8	8.3	5.9
0.30	20.4	14.4	10.2
1.00	37.3	26.4	18.6

*Numbers used for Galileo Probe separation mechanism

9.3.3 *Initial laser signal acquisition*

An initial acquisition mode will occur after propulsion module separation to align the three spacecraft and their instruments in their proper configuration. The first step of initial acquisition will require the spacecraft to achieve a pointing control of ±5 arcsec which includes a pointing knowledge of ~±2 arcsec from the star trackers. The 5-arcsec pointing control capability will be provided by the FEEP μN thrusters, which are the only method of attitude control after separation from the propulsion module.

Once this is achieved, ground stations will uplink the approximate relative attitudes of each spacecraft for their use in laser beam pointing and acquisition of each other.

During initial acquisition, the laser beams from all three spacecraft are defocused to roughly 10 times the diffraction-limited diameter. The signals from the quadrant detectors should then all be easily detectable, and can be used to control the spacecraft attitudes at least an order of magnitude better than assumed with the star trackers. Once acquired by the quad-detectors, the laser beams are refocused to give nearly diffraction-limited performance, and the normal accuracy of the optical direction measurement systems should be achieved.

The 2-arcsec pointing knowledge in three axes will be provided by an attitude determination system consisting of multiple star cameras with signal processing and attitude determination algorithms in the spacecraft central computer. A total of four star cameras will be on each spacecraft. This will ensure that two cameras will always have enough available bright stars (approximately 40 to 200 stars per camera) for pattern correlation and Kalman filtering to obtain the high precision at a 1-Hz rate. Since the spacecraft does a 360° rotation around its symmetric body axis once per year (orbit), each star camera will be pointed normal to the ecliptic plane twice a year where bright star availability is limited.

Two star cameras are required to be functioning simultaneously to meet the pointing knowledge requirement in all three axes. Each star camera can only meet the pointing knowledge requirement in two axes (camera boresight pitch and yaw). The third camera axis (boresight

roll) greatly exceeds the requirement, and therefore must be compensated by a second camera. Essentially, the information of the roll axis of camera 1 will be supplemented by the pitch and/or yaw axis of camera 2 so long as the both boresights do not have a similar pointing vector.

The IRU may or may not be in use during this phase of the mission.

9.3.4 Normal operation with three interferometer arms

For attitude control, the roll axis is taken to be along the bisector of the axes for the two optical systems on the spacecraft. Pitch is the motion of that axis perpendicular to the interferometer plane, and yaw is the motion of the axis in the plane. Pitch, yaw, and roll can be controlled using signals from the quadrant detectors for the two optical systems. The difference of the yaw signals from the two quadrant detectors also will be used to control the angle between the primary and secondary axes. The attitude control requirements for LISA for pitch, yaw, and roll are as follows: 30 nrad for 1 s period, 10 nrad for 10 s, 3 nrad for 100 s, and 1 nrad for 1000 s.

For translation (position) control, the average of the outputs from the two inertial test-mass sensors in each spacecraft will be used to control the positions of the spacecraft. The LISA requirements are 3 nm for 10 s period, 1 nm for 100 s, 0.3 nm for 1000 s, and 0.1 nm for 10,000 s. The differences of the signals from the two inertial test-mass sensors will be used by the payload to apply small forces to the test masses via the capacitive plates to keep the test masses near the centers of their housings.

(Note: all measurement accuracies and requirements are given as 1 sigma.)

9.3.5 Operation with two interferometer arms

For two-arm operation, the spacecraft at the intersection of those two arms will be called the primary spacecraft. If all six optical direction sensor systems are operating, the attitude control systems would use the same method as discussed above. However, if only the four optical direction sensor systems looking along the two operating arms are available, another source of information on roll of the two secondary spacecraft about the operating arms is needed. Fortunately, the roll control requirements for the secondary spacecraft in this case are a factor 10,000 less severe than for three-arm operation.

The most sensitive alternate roll information can be obtained from differencing the outputs from the two inertial sensor systems on each spacecraft, if both are working. However, long-term drift would need to be corrected using information from the star trackers. If only one inertial sensor system is working, the short term roll information would have to come from the apparent rotation of the test mass inside its housing. The star trackers would still be used for longer time scales.

9.4 FORCES AND TORQUES ON THE SPACECRAFT

The solar radiation pressure force on each spacecraft is expected to be in the range of 0.02 to 0.03 mN. The fluctuations in the force along each axis are estimated to be 3, 2, 1.5, and 1 nN respectively at periods of 10, 100, 1000, and 10,000 s. These fluctuations will be due to variations in both the solar luminous intensity and the solar wind.

For torques, the steady value is expected to be roughly 3 mN-m for the axis of maximum torque. The fluctuations in torque about each of the three axes are estimated to be 1, 0.7, 0.5, and 0.3 nN-m respectively at periods of 1, 10, 100, and 1000 s. This includes the effects of variations in magnetic torque, as well as in the solar luminous intensity and the solar wind.

Tables 9-2 and 9-3 contain the precision of the angular information and the relative position produced by the science payload.

According to the science team, the star cameras can operate at an update rate of 1 Hz during the science mode since no major disturbances are expected at this bandwidth. Again, two cameras will be used to meet the pointing knowledge in all three axes.

The science team has decided that high-bandwidth IRU information to accurately propagate the attitude between 1 Hz star updates is not necessary (i.e., to determine attitude motion in the spectral region >0.5 Hz at the Nyquist frequency of the star tracking). Therefore, the IRU will be powered off after initial acquisition. The IRU can be powered on at any time deemed necessary during the course of the mission.

Table 9-2 Science payload angular information capability.

Measurement Duration (s)	Angular Information (nrad)
1	3.0
10	1.0
100	0.3
1000	0.1

Table 9-3 Science payload relative position information capability.

Measurement Duration (s)	Relative Position (nm)
10	0.30
100	0.10
1000	0.03
10000	0.01

9.5 ADCS DESIGN

9.5.1 Attitude determination

Attitude determination sensors will consist of coarse Sun presence sensors, fine Sun sensors, star cameras, inertial measurement (or reference) units, and the science instrument.

The fine Sun sensors baselined each have a 128°×128° field-of-view (FOV) and can provide attitude knowledge of 0.017° in two axes. These fine Sun sensors have flown on various NASA, U. S. Air Force, and Comsat spacecraft. They are ideal for this mission since these sensors can be placed to constantly face the Sun throughout the entire lifetime of this mission during which they are always ≥30° off of sunline. They also provide a sanity check for the star cameras.

The star cameras baselined have 22°×16° FOV and can provide attitude knowledge of almost 2 arcsec in two axes and 16 arcsec in their boresight roll axis. Star processing at an update rate

of 1 Hz will require 8 Mips (million instructions per second) of throughput from the flight computer. Therefore, two cameras operating simultaneously will require 16 Mips, which can be satisfied by the CDS computer. This star camera's first flight will be in 1997 on the Danish Ørsted satellite. It is currently baselined for the Pluto Express and Europa Orbiter missions, too.

The IRU baselined in this study consists of three fiber-optic gyroscopes, three accelerometers, and its own processor. The bias stability of the IRU is 0.2°/h. An equivalent IRU without the accelerometers may be used in place of the baselined system. The baselined IRU has flown on Clementine, and a similar rad-hard version (25 krad) will fly on Deep Space-1 (DS-1). This IRU will be powered off during science mode with the option to be turned on at any time deemed necessary. The science team was made aware of the susceptibility to radiation of the fiber-optic gyros. Even though this may degrade the performance or render the units useless over a 10-year mission, the science team has decided to baseline this IRU. A higher precision ring-laser IRU was initially chosen to meet the above condition as well as to provide precision rate information at greater bandwidths than 1 Hz (star camera update rate) continuously during science operations. After some debate, the science team also decided that there would be no disturbances at frequencies higher than 1 Hz and that the higher bandwidth/precision IRU would not be necessary to meet the goals of this mission.

The science instrument focal plane quad-detectors will be the primary attitude reference after the initial three-spacecraft formation acquisition. The precision of the angular information will be between 0.1 nrad and 3.0 nrad. Relative position information (translation) will be provided by the science instrument with a precision between 0.01 nm to 0.3 nm.

A redundant pair of interface electronics placed on multi-chip modules (MCMs) will allow the attitude determination hardware communicate with the spacecraft Command and Data System (CDS). The interface electronics do not have their own processor.

9.5.2 Attitude and articulation control

The propulsion module will perform all attitude control prior to propulsion module separation. A redundant pair of propulsion valve drive electronics placed on MCMs will allow the spacecraft CDS computer to control the hydrazine thrusters. Each xenon-ion engine will be gimbaled and can provide pitch and yaw control. ADCS will provide actuators, drive electronics, control algorithms, and software for articulating the solar arrays. ADCS is responsible for all algorithms, analysis, software, and integration and test related to spacecraft control and maneuvers with this thruster system.

Two solar array actuators will provide the solar arrays on the propulsion module one axis of articulation. A redundant set of drive electronics located on MCMs will communicate with the CDS computer via the interface electronics. ADCS is responsible for all algorithms, analysis, software, and integration and test related to pointing these solar arrays.

The FEEP thrusters will perform all spacecraft attitude control functions after propulsion module separation. The drive electronics of the 24 FEEP thrusters have not been bookkept by the ADCS (as instructed by the science team). ADCS is responsible for all algorithms, analysis, software, and integration and test related to spacecraft control with this thruster system. Four FEEP thrusters will be located in six clusters mounted on the spacecraft. Each thruster will deliver up to 100 μN of thrust with a noise level of 0.1 μN at periods up to 10,000 s.

The two HGAs will each be articulated in one axis. The Structures and Mechanisms System will provide the actuators and ADCS will provide the drive electronics which will be placed on MCMs. The drive electronics will communicate with the CDS computer via the interface electronics. ADCS is responsible for all algorithms, analysis, software, and integration and test related to pointing these antennas.

Figure 9-1 shows a functional block diagram that also indicates the ADCS interfaces with the Propulsion System, Instrument System, and the CDS System. Table 9-4 is a mass and power estimate summary of this subsystem.

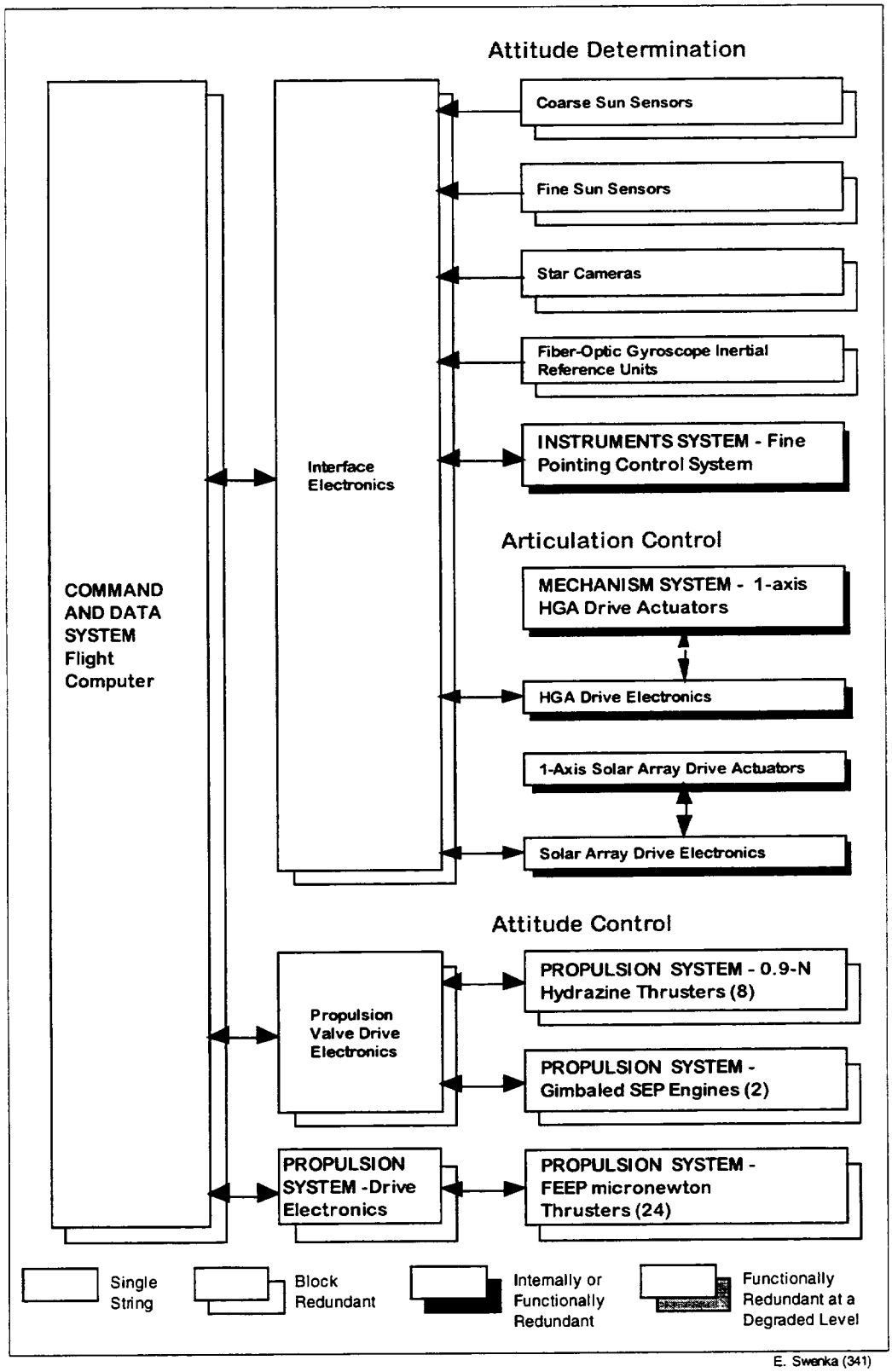

Figure 9-1 Block diagram for Attitude Determination and Control System.

Table 9-4 ADCS hardware mass and power component summary for SEP option.

Equipment Type	Location	Unit	Mass (kg)	Power (W)				Comments
				Max	Science	Cruise	Launch	
Fine Sun Sensors	S/C	2	1.28	0.50	0.50	0.50	0.50	128°x128° FOV. 0.02° accuracy. Commercial heritage.
Star Cameras	S/C	4	2.00	1.00	1.00	0.50	1.00	2-arcsec pitch and yaw. 16 arcsec boresight roll. Ørsted/Pluto Express heritage.
Inertial Reference Units	S/C	2	1.40	10.00	0.00	10.00	10.00	Fiber optic gyros. 0.2°/h bias stability. Clementine/ DS-1 heritage.
Coarse Sun Presence Sensors	S/C	10	0.10	0.00	0.00	0.00	0.00	Simple silicon photodiodes to provide 4-p steradian coarse coverage.
Interface Electronics	S/C	2	0.20	0.10	0.10	0.10	0.10	MCM. DS-1/2/3 heritage.
Propulsion Valve Drive Electronics	PM	2	0.20	0.10	0.00	0.10	0.10	Valve drivers for Propulsion Module. MCM. DS-1/ Pluto Express heritage.
Solar Array Drive Actuators	PM	2	3.40	20.00	0.00	0.50	2.00	One-axis stepper motors. Commercial heritage.
Solar Array Drive Electronics	PM	2	0.80	4.00	0.00	0.50	0.50	MCM. DS-1/2/3 heritage.
HGA Antenna Drive Electronics	S/C	2	0.80	0.50	0.50	0.50	0.50	MCM. DS-1/2/3 heritage.
Shielding			0.00					
TOTAL		28	10.18	36.20	2.10	12.70	14.70	

Legend:

MCM multi-chip module
PM propulsion module
S/C spacecraft

9.6 ADCS COST

Table 9-5 gives a cost breakdown for this subsystem. Please note that this cost estimate is for a single spacecraft. These costs include the following assumptions and responsibilities:

- The Instrument System will be responsible for providing the science instrument sensor signal processing algorithms that will produce three-position (translations) and three-angular (rotations) digital outputs to ADCS. ADCS will be responsible for implementing all spacecraft and payload pointing and translation control algorithms and related software in the spacecraft computer.
- In a like manner, the Instrument System will provide all instrument error analyses, in-flight instrument calibration algorithms, in-flight test-mass electrostatic charge removal algorithms, and supporting six-degree-of-freedom dynamic simulations of the science instrument with its internal electrostatic force-rebalance test-mass capture loops.
- Spacecraft bus may be adapted from a commercial bus, but the ADCS must be customized.
- Spacecraft will have inheritance from other existing and planned NASA/JPL missions.

- DS-1 autonomy (remote agent).
- Star camera from Pluto Express and Europa Orbiter.
- IRU from Clementine and DS-1.
- Star Identification, attitude estimation, inertial vector propagation, and fault protection software and algorithms from Pluto Express and Europa Orbiter.
- MCM electronics for interfacing and propulsion driving from DS-1, DS-2, DS-3, Pluto Express, and Europa Orbiter.
- Some ground support equipment will be inherited from Pluto Express/Europa Orbiter, DS-1, DS-3, and Mars Pathfinder.
- New methods, hardware interfacing, algorithms, and software costs that cannot be inherited.
- Spacecraft attitude and translation sensing, determination, and control in the nanoradian/nanometer range through use of the science payload and FEEP thrusters.
- Guidance and control methods and algorithms for three-spacecraft constellation deployment and orbit insertions, formation acquisition, and orbit maintenance.
- Structures and Mechanism will provide HGA actuators.
- ADCS will supply the following for solar array articulation.
  - One-axis rotary actuators.
  - Solar-array drive electronics.
  - Software and control algorithms.
- Propulsion will provide power conditioning /drive electronics for FEEP thrusters.
- ADCS will provide subsystem level integration and test of any hardware embedded in the ADCS software and controls (i.e., payload, HGA actuators, and FEEP thrusters).
- No non-recurring costs for flight hardware, spares, and engineering models.
- Includes costs for contract monitoring.
- 30-month Phase C/D.

Table 9-5 ADCS cost estimate for SEP option.

Component	Cost Estimate (FY'97$K)
System engineering	681
Controls and analysis	1,686
Software	2,481
Integration and test	6,473
Ground system engineering	1,960
Hardware engineering	2,649
Flight hardware	6,572
Flight spares and engineering models	1,752
Total	24,252

SECTION 10—COMMAND AND DATA SYSTEM

This section describes and estimates for the Command and Data System. The estimate includes mass, power, volume, and costs. The estimated software costs cover only the command and data handling functions and integration of software provide by other subsystems.

The spacecraft controller consists of two identical units operating in a String A and String B fashion. String B acts as a warm backup and receives state data from String A at specified intervals. String B will contain a watchdog timer to monitor String A. If this timer runs out, String B will take over as the primary spacecraft controller. This document describes the interfaces to each unit at a functional level concentrating on I/O (input/output) traffic and how the traffic affects the design of the spacecraft controller. The mission requirements that impact the design of the spacecraft controller are listed in Table 10-1.

Table 10-1 Relevant mission parameters.

Mission Parameter	Description
Orbit	Sun elliptical, 1-AU, 20° behind Earth (150 and 52×10^6 km)
Primary Mission Duration	1-year cruise, 3-year operation
Additional Extended Mission	7 year
Redundancy Required	Block redundant required for 10-year mission
Spacecraft Required	Three in triangular array
Data Transfer	Each spacecraft sends and receives continuously from other two spacecraft
Launch Vehicle	Single Delta II 7925 or 7925 H
Technology Cutoff Date	2000
Target Launch Date	2005
Phase C/D Duration	24 months
Telecom Uplink Rate	2 kbps
Telecom Downlink Rate	7 kbps
Downlink Period	1 per week
Number of Instruments	One per spacecraft
Science Data-Taking Schedule	Continuously acquired
Data Latency	<7 days
Data Criticality	Gaps ≤1/week acceptable
Science Data Input Rate(s) Raw Compressed	Each spacecraft 1000 bps 200 bps
Science Data Processing Requirements	5:1 formatting required
Science Data Volume (Memory)	121 Mbits
Telemetry Data Rate Instrument Spacecraft	 100 bps 100 bps
Telemetry Data Volume	121 Mbits
Mass Limitations	200 kg/spacecraft
Power Limitations	25 W for CDS
Radiation (Total Ionizing Dose)	Solar radiation at 1 AU (150×10^6 km) 5.4 krad/year with 0.25 cm Al RDM=2 (Total 54 krad for 10-year mission)
Power Source	Solar cells

10.1 SPACECRAFT CONTROLLER

The spacecraft controller will perform the command and data handling functions, attitude determination, and control functions as well as processing science data. These functions include science and engineering data collection and data storage. Power to the controller will be supplied by the spacecraft. The functional interface diagram is shown in Figure 10-1. The spacecraft controller hardware configuration is shown in Figure 10-2.

The Mars Surveyor Program flight computer is suggested for this mission. The Lockheed-Martin RS 6000 flight computer contains 128 Mbytes of DRAM and 3 Mbytes of PROM. The relatively low data rates for science and telemetry permit all data to be buffered and stored in DRAM on the flight computer board. This eliminates the need for a separate mass memory board, thereby reducing the subsystem mass and power. This data storage architecture was used on the Mars Pathfinder mission.

Subsystem command, control, and monitoring will be executed via the hardware interfaces indicated in Table 10-2.

The ADCS controls and monitors various attitude reference devices, determines spacecraft attitude, and issues commands to control the attitude of the spacecraft.

10.2 DATA HANDLING SYSTEM

The Data Handling System is required to perform many critical spacecraft functions. Several examples are as follows:

- Uplink command processing and distribution.
- Sequence storage and control.
- Maintenance and distribution of spacecraft time.
- Collection and formatting of engineering spacecraft sensor data.
- Bulk storage of science and engineering data.
- Subsystem control and services.
- Spacecraft system control services (non-attitude control).
- Spacecraft fault protection.
- Reed-Solomon downlink.

Table 10-2 Mission-specific controller interfaces.

Specific Interface	Item
Attitude Determination	Fine Sun Sensor (2)
	Coarse Sun Presence Sensors (10)
	Star Tracker (4)
	IRU (2)
	Interface Electronics (2)
Articulation Control	HGA Drive Actuators (2)
Attitude Control	Propulsion Module Interfaces (2)
Science	Instruments (1 per spacecraft)
Telecom	Uplink: 2 kbps
	Downlink: 7 kbps

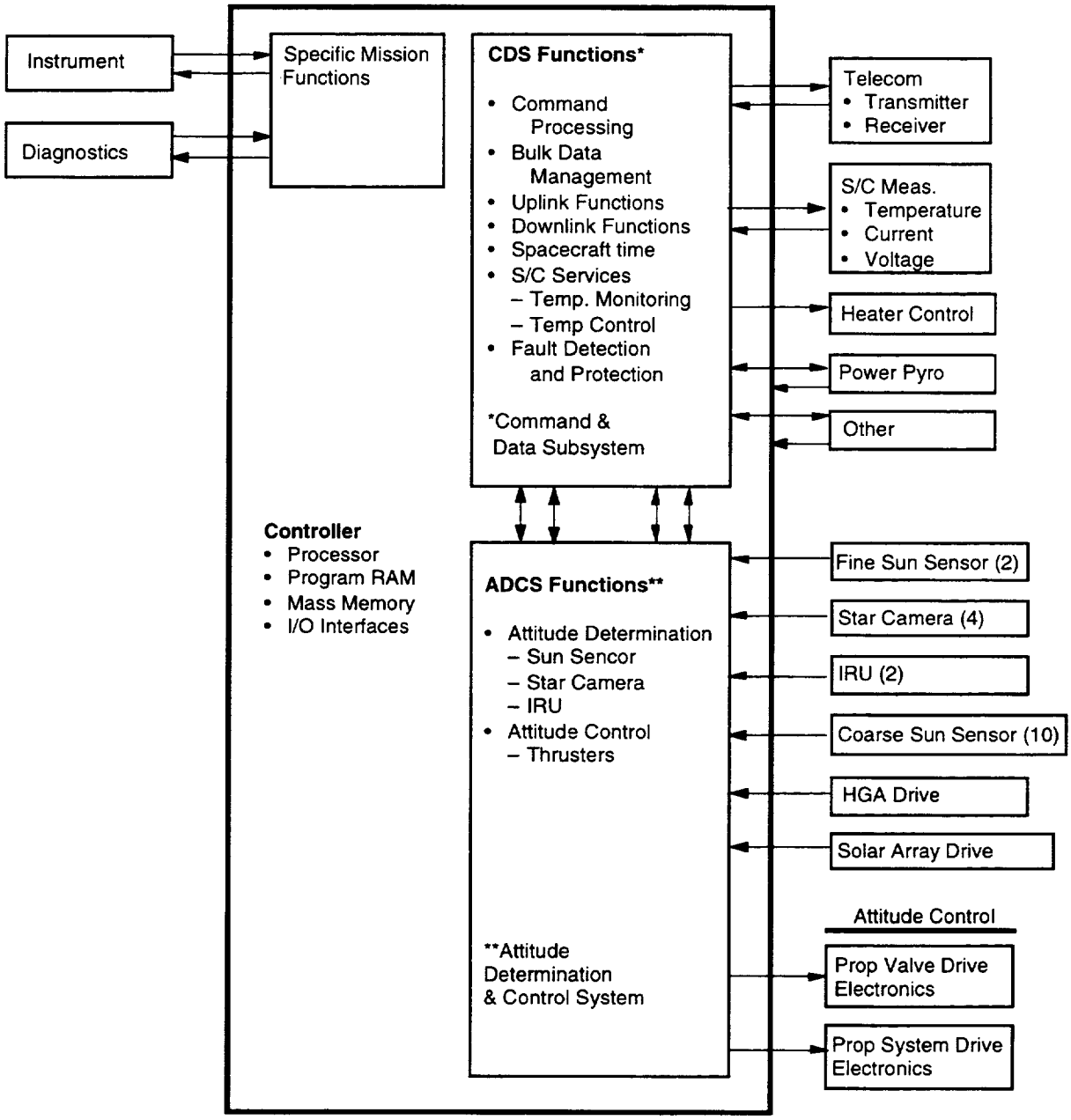

Figure 10-1 Spacecraft controller functional interface diagram.

10.3 RADIO FREQUENCY SYSTEM INTERFACE

The spacecraft controller communicates to the Radio Frequency System (RFS) with two different interfaces. The first interface provides data to be downlinked to the RFS as well as receiving uplinked communications from the RFS. The second interface connects to the RFS controller. The RFS controller receives commands from the controller. The commands place the RFS into different modes (mode control). In turn, the RFS provides telemetry data to the controller. The controller is responsible for decoding the uplink packets as well as generating the downlink packets.

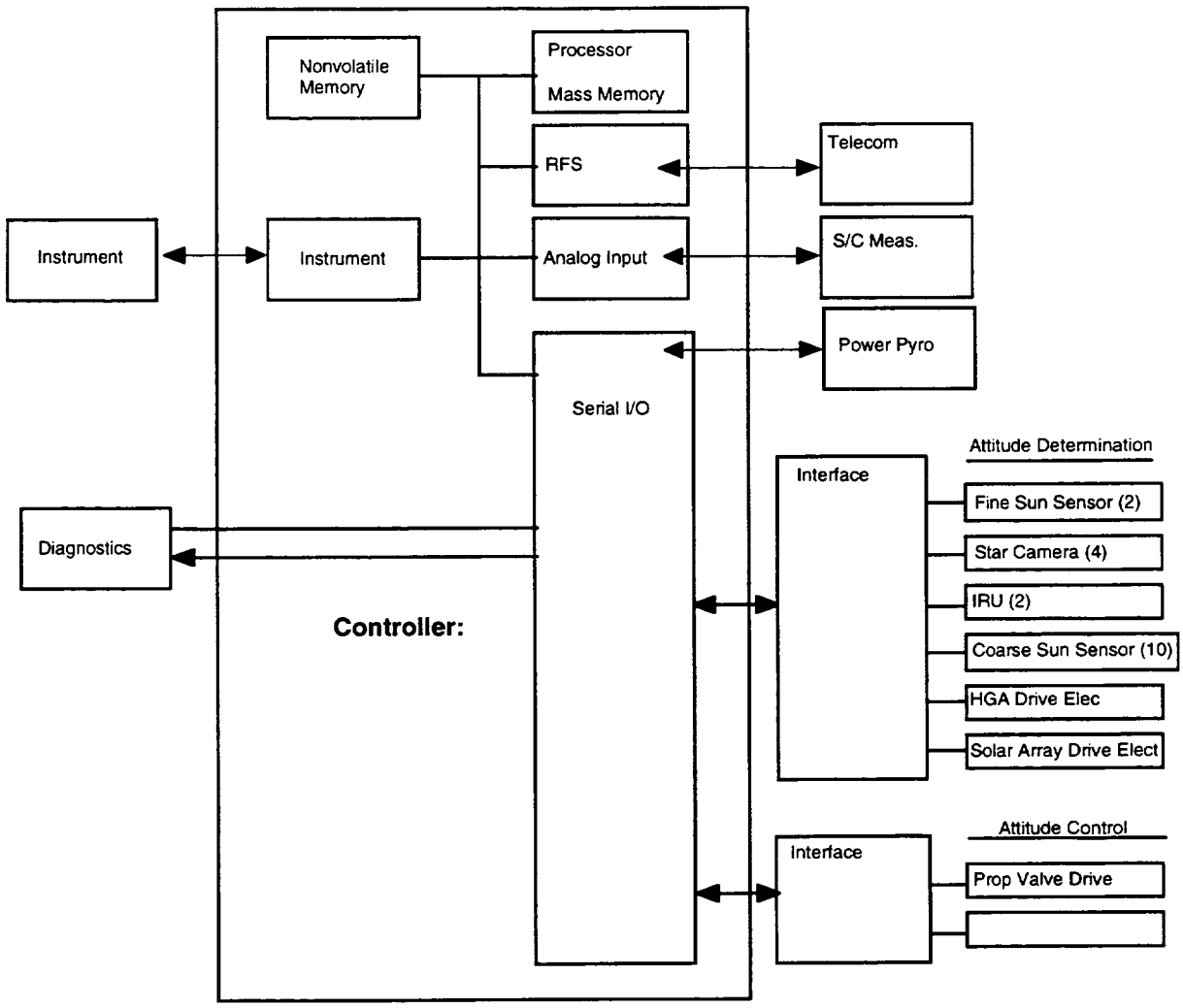

Figure 10-2 Spacecraft controller configuration.

10.4 FLIGHT SOFTWARE

The software interface diagram is shown in Figure 10-3. The controller will be able to use a commercially available operating system and will be programmable in a high-level language such as C or C++.

The controller will host software for the spacecraft. If a subsystem such as science needs to have the controller perform specific functions, then the science team will provide the software to the CDS team.

The CDS team will coordinate the software interfaces so that the capabilities of the controller (Mips, memory, scheduling) are not exceeded. The CDS team will also integrate the delivered software with the other software elements before spacecraft integration.

The spacecraft controller will host software tasks that have been developed by several systems besides the CDS. These include

CDS: Controls critical spacecraft functions, acts as the "switchboard" routing messages and hosts the spacecraft fault protection.

ADCS: Software for the spacecraft attitude determination and control.

RFS: Performs downlink encoding on the data stream.

Science: Software will be developed to command the science controller and to collect the science data.

GDS: The Ground Data System (GDS) will be developing software for autonomous sequencing.

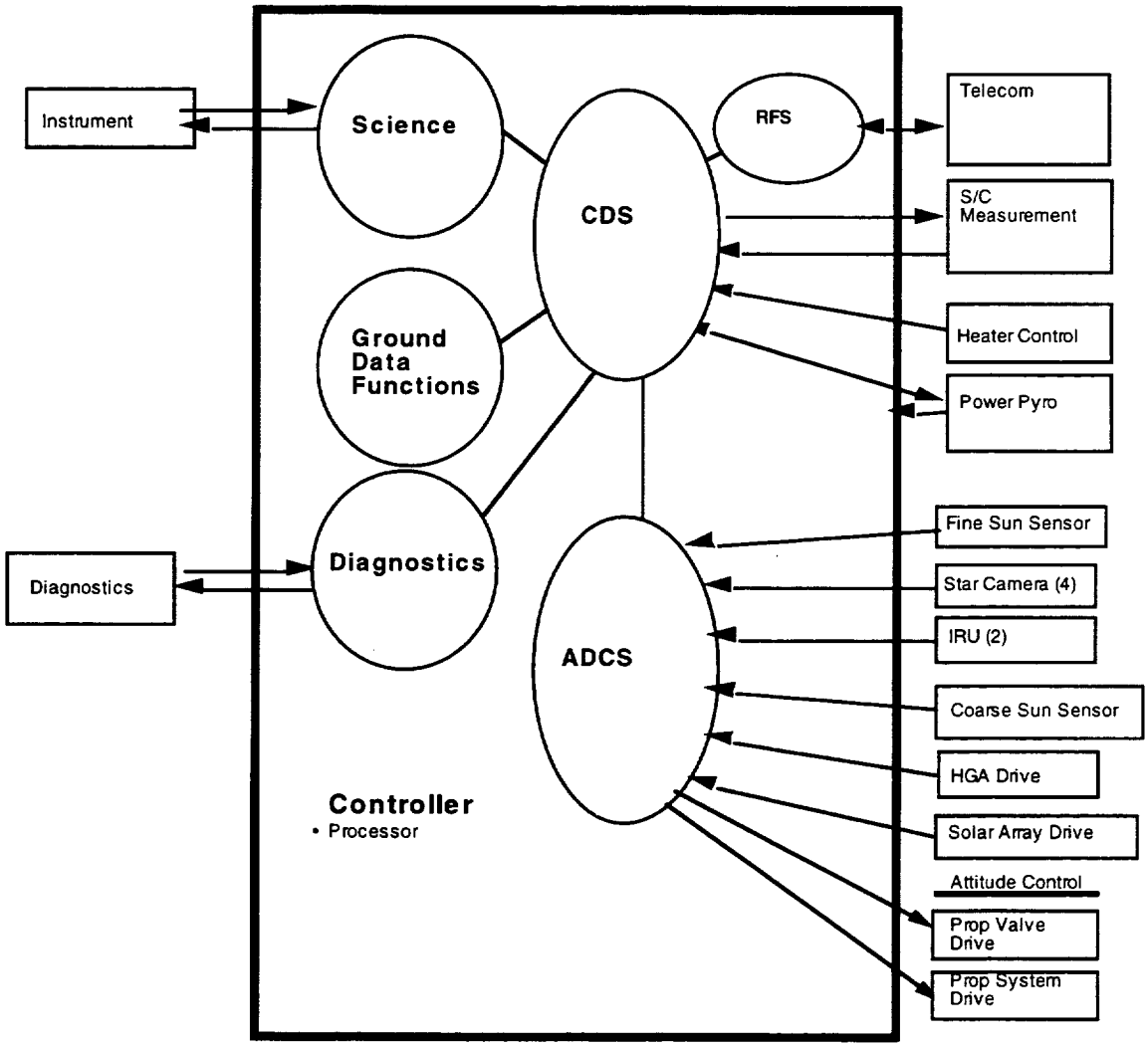

Figure 10-3 Software interface diagram.

10.5 MASS, POWER, AND COST ESTIMATE

The mass, power, and flight hardware recurring engineering estimates are shown in Table 10-3. The workforce breakdown is given in Figure 10-4. An estimated cost profile based on Phase B and C/D durations, intended only to provide a rough estimate for Phase A planning purposes, is shown in Table 10-4 and Figure 10-5.

The cost estimation for non-recurring costs are made with the following assumptions:

- The spacecraft controller is block-redundant.
- High inheritance from previous programs.
- Previously designed flight hardware is used as much as possible.
- Some new ground support equipment required. As much as possible, equipment is reused from previous programs.
- Some new ground support software required. As much as possible, software is reused from previous programs.
- One breadboard and an engineering model is costed. Use of existing common project lab equipment (Flight System Testbed) is assumed to be available for development purposes.
- Cost estimates do include JPL burden.
- New documentation will be minimal, red-lined documentation where required.
- Whenever possible, subsystem qualification will be performed by analysis, based on high flight inheritance.
- Software costs only include CDS capabilities as well as costs to integrate software from other systems.
- ADCS-, science-, and GDS-related costs of hardware and software are not included in these costs.
- The cost for quality assurance and reliability will be carried by the project.
- Assembly, test, and launch operations (ATLO) costs not included.
- The cost or mass of external cabling is not included.

It has been assumed that all the required functional designs will have been developed for previous programs. An additional cost of $1.2M, not included in the cost estimates, may be needed if LISA is the first mission to use these boards.

Table 10-3 LISA CDS mass, power, and cost.

		Unit	Mass (kg)	Power/ Unit (W)	Cost ($K) Recurring	Cost ($K) Develop	Power (W) Science	Power (W) Cruise	Power (W) Launch	NASA TRL	Comments	Heritage
Total			14.5	13.1	1,066.0	1,200.0	13.1	9.9	9.9	6		
Processor	VME, RS/6000 22 Mips—Ver 2, Lockheed Martin	2	2.30	15.60	800.0		15.60	9.36	9.36	8	128-Mbytes DRAM, 3-MB EEPROM	Stardust
VME, Board	VME, Up/Downlink	2	1.80	2.00	44.0	250.0	2.00	2.00	2.00	6	Proposed FDSE:2.057	Proposed
VME, Board	VME, Analog/Digital Input Bd	2	4.00	3.00	84.0		3.00	3.00	3.00	8	Estimated Board	SeaWinds
VME, Board	VME, xStrap Board	2	1.80	1.50	40.0	500.0	1.50	1.50	1.50	5	Cross-strap between String A and String B	Proposed
VME, Board	VME, Chassis, Composite	2	1.80		10.0	100.0				8	Proposed development by Lockheed Martin	Mars Penetrator
VME, Board	VME Serial I/O board	4	1.80	4.00	88.0	350.0	4.00	4.00	4.00	5	8-channel card RS422,485. or 232. 8-Mbps max rate for 422 or 485. 100-Kbps for 232.	
Solid State Memory											Use DRAM available on flight computer board	
Shielding (kg)				1.0								

Estimated Subsystem Cost ($M FY95) **12.0**

Additional Potential Development Costs

Development costs are based on the maturity of and required parts for each board. Typical development costs include design, breadboard, test, flight qualification, and configuration control. Documentation includes, requirements, specifications and user manuals. If this mission is the first user for new development, the potential added cost is estimated to be: **1.2 ($M)**

Hardware Recurring Calculation

Unit	Number	Cost/Unit	Subtotal
Flight H/W	3.0	1,066	3,198.0
Spare	0.5	1,006	533.0
EM	1.0	711	710.7
Breadboard	1.0	267	266.5
Lab Prototype	2.0	133	266.5
Total Recurring Cost			4,974.7
			1,510.2 Spares

Summary		
H/W Recurring Cost	5.2	$M
Estimated Workforce	6.7	$M
Estimated Total Cost	12.0	$M
Estimated Volume	14.9	Liters
Estimated RAM Req.	28.4	Mbytes
Estimated Mass	14.5	Kg
Processor Performance	22	Mips

Table 10-4 Estimated CDS cost profile.

	2000	2001	2002	2003	2004	Inflated Est.
Hardware Procurements	588	1,176	2,726	1,372	193	6,055
Workforce	288	668	2,216	2,837	1,864	7,873
Annual Totals	876	1,844	4,941	4,210	2,057	13,928

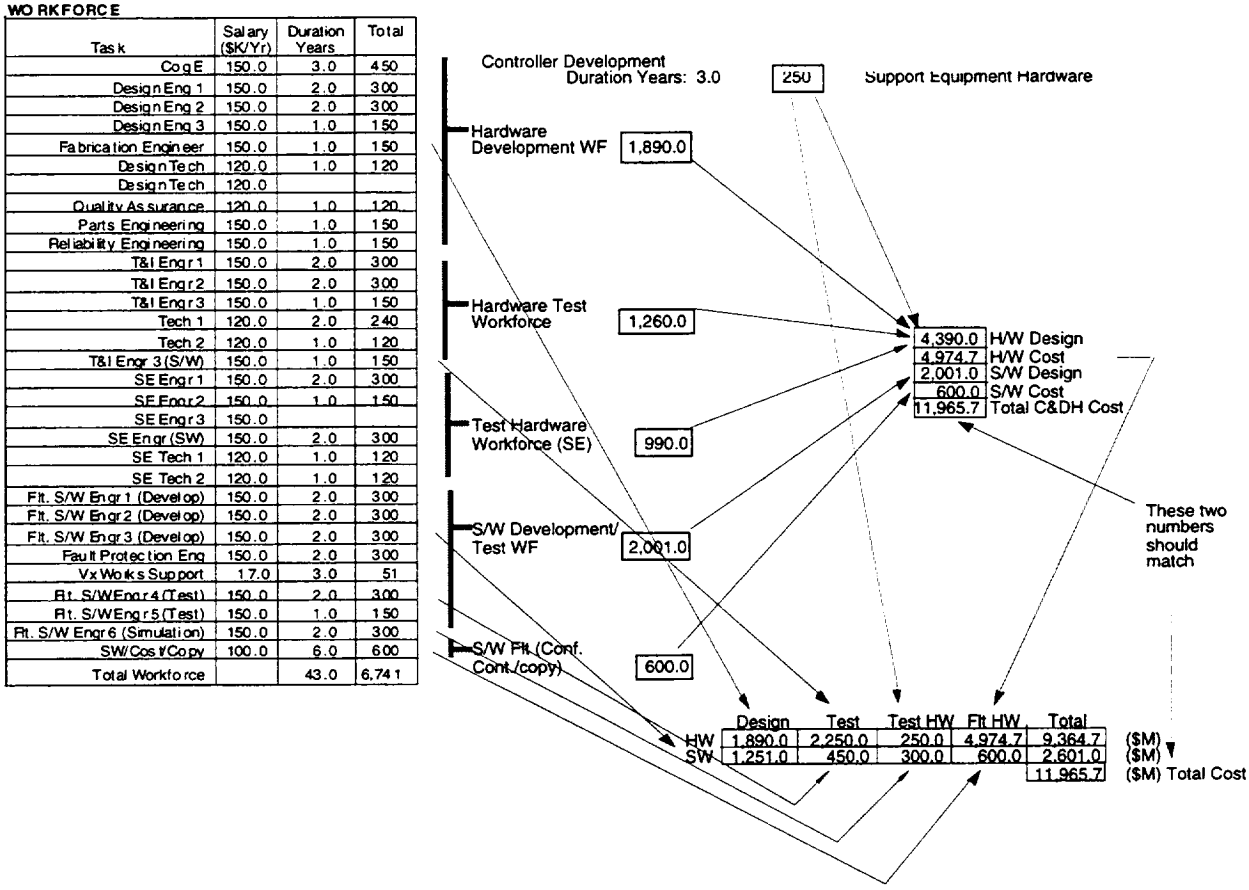

WORKFORCE

Task	Salary ($K/Yr)	Duration Years	Total
CogE	150.0	3.0	450
Design Eng 1	150.0	2.0	300
Design Eng 2	150.0	2.0	300
Design Eng 3	150.0	1.0	150
Fabrication Engineer	150.0	1.0	150
Design Tech	120.0	1.0	120
Design Tech	120.0		
Quality Assurance	120.0	1.0	120
Parts Engineering	150.0	1.0	150
Reliability Engineering	150.0	1.0	150
T&I Engr 1	150.0	2.0	300
T&I Engr 2	150.0	2.0	300
T&I Engr 3	150.0	1.0	150
Tech 1	120.0	2.0	240
Tech 2	120.0	1.0	120
T&I Engr 3 (S/W)	150.0	1.0	150
SE Engr 1	150.0	2.0	300
SE Engr 2	150.0	1.0	150
SE Engr 3	150.0		
SE Engr (SW)	150.0	2.0	300
SE Tech 1	120.0	1.0	120
SE Tech 2	120.0	1.0	120
Flt. S/W Engr 1 (Develop)	150.0	2.0	300
Flt. S/W Engr 2 (Develop)	150.0	2.0	300
Flt. S/W Engr 3 (Develop)	150.0	2.0	300
Fault Protection Eng	150.0	2.0	300
Vx Works Support	170	3.0	51
Flt. S/W Engr 4 (Test)	150.0	2.0	300
Flt. S/W Engr 5 (Test)	150.0	1.0	150
Flt. S/W Engr 6 (Simulation)	150.0	2.0	300
SW Cost/Copy	100.0	6.0	600
Total Workforce		43.0	6,741

Figure 10-4 CDS workforce breakdown.

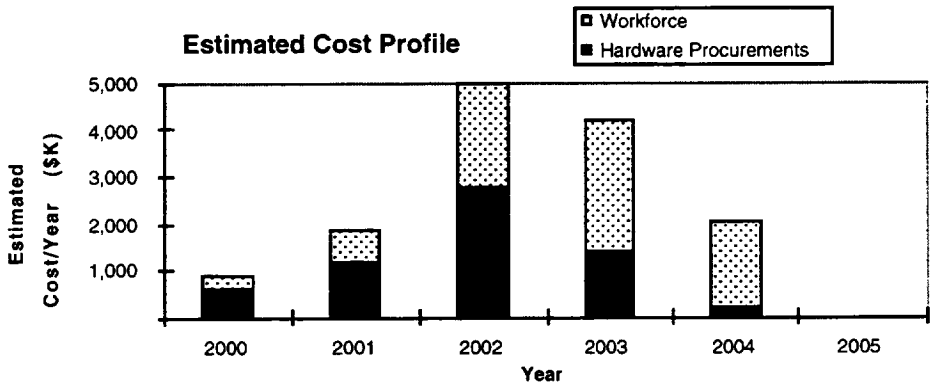

Figure 10-5 Estimated CDS cost profile.

In order to refine the design for mass memory, processor type, clock rate and such, further discussions must be held on the following topics:

- Reliability
- Spacecraft clock accuracy
- Total ionizing dose radiation
- Single-event upset rate
- Parts classifications

10.6 NEW TECHNOLOGIES REQUIRED

This estimate is based on the development of technologies to meet the mass, volume, and power values listed. The list of technologies is shown below:

- Miniaturization of flight electronics
- A flexible architecture which provides for little or no engineering development
- Development of general purpose multi-mission ground support equipment
- Development of flight multi-mission software to allow for small amount of mission specific code
- Receivables/Deliverables

10.7 RECEIVABLES AND DELIVERABLES

The following items are to be delivered to the project:

Documentation
- Functional interface document
- Controller specification document
- Hardware interface documents for each controller I/O connection
- Controlled design document
- User's handbook (hardware)
- User's handbook (software)
- Flight unit test reports
- Software functional interface document
- ATLO integration and Ops procedures
- Instrument hardware/software interface agreements

Hardware
- Engineering model controller
- Flight unit controller
- Controller support equipment

Software
- Prototype CDS software
- Beta CDS software
- Flight CDS software

The following items need to be received:

Documentation

- Controller requirements (mass, power, volume, Mips, memory, data rates, fault protection, etc.)
- Spacecraft interface document (data rate, format, mode, commands, telemetry)
- Environment requirements (lifetime, radiation, vibration, pyro-shock, etc.)
- Schedule and funding profiles
- Test requirements (performance characteristics)
- Instrument hardware/software interface agreements

Hardware

- Instrument interface simulator/breadboard
- Spacecraft interface simulator/breadboard

Software

- Operating system source code
- Compiler
- ADCS flight software
- Science flight software
- Thermal control algorithms
- RFS control/encoding algorithms
- Specific interface test code

SECTION 11—POWER

Each LISA spacecraft will consist of two modules: a sciencecraft, and a propulsion module jettisoned at end of cruise. The sciencecraft is a flat cylinder, 1.8 m in diameter by 0.5 m thick. An external "sunshade" is added to the outer sciencecraft edge on the Sun side. This shade combined with the nominal sciencecraft flat surface provides a total Sun-facing diameter of 2.2 m with a total surface area of 3.80 m^2. The surface area of the central science is 1.8 m^2. The orbital configuration allows the sciencecraft to be in Sunlight at all times, with a maximum off-Sun angle of 30° (during science operations). Sun-facing surfaces are expected to reach 80° C.

The power subsystem design is based on the following technologies:

- GaAs solar-cell technology at 19% efficiency for power generation for both the sciencecraft and SEP arrays.
- Lithium-ion batteries for power storage based on 80-Wh/kg specific energy density and 140-Wh/l volumetric density.
- Integrated multi-chip module to VME boards for power control, management and distribution, and laser pyro drivers. This technology is based on expected development prior to the technology cut off of FY 2001. Expected mass and volume of 300 grams per power element slice, and 150-cc per element slice.

The mission power and energy requirements for the sciencecraft are shown in Tables 11-1 and 11-2. The power requirements for the science mode drive the subsystem design. Cruise power for the hydrazine thrusters can be supported by the flat body mounted sciencecraft solar array. Launch power will be supported by a secondary battery. The battery will provide fault protection during flight.

A 20-Ah Li-Ion battery will support launch for 2.7 hours. During this time launch, separation and deployment, and Sun acquisition will occur. The launch cycle depth of discharge is 80% with few expected cycles expected thereafter. Data on the battery is given in Table 11-3. A single body-mounted GaAs solar array of 1.57 m^2 surface area and a mass of 2.15 kg supplies the power for the sciencecraft. This array is fixed to the Sun-facing outer edge of the sciencecraft and is sized for a 30-degree off-Sun angle. Array data is presented in Table 11-4 for end-of-life after the 4-year nominal mission.

The power electronics system will use four elements. These elements are the Power Management Unit, the Power Control Unit (including the battery charger), and two laser Pyro Switching Unit slices. The power subsystem mass is based on 100 W/kg and 237 W power. This system is estimated to have a mass of 2.9 kg. The estimated cost of the spacecraft power system for one spacecraft is given in Table 11-5.

Table 11-1 Power requirements.

Power Mode	Science	Propulsion	Launch
ADCS Power (W)	2.1	11.7	12.2
CDS Power (W)	13.1	13.1	13.1
Instruments Power (W)	72.2	0.0	0.0
Propulsion Power (W)	0.0	17.8	28.1
Power Subsystem (W)	0.0	27.0	0.0
Structures Power (W)	0.0	0.0	0.0
Telecom-S Power (W)	18.4	4.0	18.6
Thermal Power (W)	0.0	17.0	17.0
Totals	105.8	90.6	89.0
System Contingency Req.	30%	30%	30%
System With Contingency:	195.1	126.6	157.2

Table 11-2 Battery requirements.

Power Mode	Power (W)	Duration (h)	Capacity (Wh)
Science	155.3	1	155.3
Propulsion	93.4	0	0.0
Launch	130.7	0	0.0
Totals		1	155.3

Table 11-3 Battery data.

Battery Technology	
Technology	Lithium Ion
Capacity (Wh)	540
(Ah)	20
Voltage	27
%Depth of Discharge (Avg)	0.8
Cycle Number (Year)	<10
Volume (ℓ)	3.38
Mass (kg)	5.91
Number of Batteries	1
Average Efficiency (%)	0.80

Table 11-4 Sciencecraft solar array.

Solar Array Technology	
Technology	GaAs
Array Power (W)	195.1
Maximum Eclipse Time (min)	0
Solar Array Cosine Losses	0.86
Solar Array (m^2)	1.57
Array Panel Type	Fixed Body Mounted
Cell Stack Mass (kg)	1.18
Substrate Mass (kg)	0.97

Table 11-5 Spacecraft power subsystem cost.

	Cost ($M)
Design	0.9
Test hardware	0.3
Testing	1.9
Flight hardware	2.6
Total	5.7

A separate array and drive electronics are added for the solar-electric propulsion module. All pyro events are conducted off the existing sciencecraft pyro drivers.

The thruster requires power supplied at 55 V with a range from 53 to 57 V. The power requirement for the SEP is 558 W (at beginning of mission). The SEP power must be conditioned before the SEP drive. Power contingency on the SEP is 5% for the existing Hughes thruster. The SEP array uses 19% efficient GaAs solar cell technology with a total surface area of 5.58 m^2 and a total mass (not including support structure and drive mechanism) of 6.97 kg. This deployed array is configured into two symmetrical panels with a single axis of freedom. The array is sized based on 100 W/m^2 specific energy density and 80 W/kg.

The SEP power electronics will use MCM technology integrated to a VME bus for power control.

Data on the SEP power subsystem are given in Table 11-6. The system is expected to have a mass of approximately 5.6 kg. The estimated cost of the SEP power subsystem for one spacecraft is given in Table 11-7, for end-of-life after the 13-month cruise phase.

Table 11-6 Solar array for the SEP engine.

Solar Array Technology	
Technology	GaAs
EOL Array Power (W)	514.5
Maximum Eclipse Time (min)	0
Solar Array Cosine Losses	1.00
Solar Array (m^2)	5.58
Array Panel Type	Two Panel, 1 Axis of Freedom
Array Mass (kg)	6.97

Table 11-7 SEP power subsystem cost.

	Cost ($M)
Design	0.2
Test hardware	0.1
Testing	0.9
Flight hardware	1.6
Total	2.8

SECTION 12—THERMAL CONTROL

12.1 INTRODUCTION

The science requirement on the Thermal Control System is that the spacecraft and its elements be extremely thermally stable. To accomplish this the spacecraft electrical power dissipation must be constant, and all elements dissipating power must operate continuously, which will keep all elements at a constant temperature. The only rapid change in external environment is the high-frequency energy fluctuations from the Sun, which are low level, and the thermal and spacecraft designs have taken this effect into account.

The Thermal Control System will use multilayer insulation, thermal surfaces, thermal shields, thermal conduction isolation, with electric heaters and thermostats. The development status of the described elements are adequate to support this mission.

12.2 SCIENCECRAFT

The sciencecraft will operate at a distance of about 20° from the Earth at 1 AU (52 and 150×10^6 km). The sciencecraft is disk-shaped, with a diameter of about 1.8 m, and a depth of about 50 cm. The inclination of the 5×10^6 km suborbit is 60° with respect to the plane of the ecliptic. Because of the orbit, the solar thermal environment to which the spacecraft is exposed is constant; there is very small variation of temperature level and stability due to the external environment.

The Thermal Control System will consist of thermal control surfaces, thermal shields, electrical heaters/thermostats, and thermal isolation to minimize temperature variation due to the small external environmental variation, and shading of the sides by the solar array to minimize thermal gradients in the structure. The thermal control surfaces will be designed to give the proper operating temperature during science operations. During the cruise phase, when the instrument is unpowered, about 17 W of heater power will be needed to keep the electronics at the proper operating temperature.

12.3 PROPULSION MODULE

The Thermal Control System for the propulsion module provides the thermal control for the structure, tanks, and hydrazine system. The thermal control will comprise multilayer insulation, thermal surfaces, and electrical heaters/thermostats. The thermal system will provide heaters for the power processor unit radiator.

The interface between the propulsion module and the sciencecraft will be developed within the sciencecraft design. The elements of this interface thermal control are thermal conduction isolation and multilayer insulation.

Table 12-1 gives the estimated mass and power for the Thermal Control System for one spacecraft. Table 12-2 gives the estimated cost of the Thermal Control System for one spacecraft.

Table 12-1 Thermal Control System requirements.

Component	mass (kg)	power (W) (cruise)
Bottom thermal shield	0.5	0
Internal shielding	0.5	0
Thermal surfaces	0.5	0
Sciencecraft heaters	0.2	17
Propulsion module insulation	2.7	0
Propulsion module heaters	0.3	17

Table 12-2 Thermal Control System cost.

Task	Cost ($M)
Design	0.3
Test hardware	0.0
Testing	0.2
Flight hardware	0.6
Total	1.1

SECTION 13—TELECOMMUNICATIONS

The mission that will allow scientists to detect gravity waves will launch three spacecraft in 2004 to go to a solar orbit at 1.0 AU (150×10^6 km) and trailing the Earth at 0.35 AU (52×10^6 km). This report describes the telecommunications subsystem necessary for this mission.

The telecom system will use X-band transmission from the satellite and have two downlink modes, one with a 7-kbps high rate to transmit science data in its normal operations mode and another with a 10-bps low rate for spacecraft health and emergencies. The DSN 34-m beam waveguide (BWG) station will receive X-band downlink, and will also uplink X-band commanding at a rate of 2000 bps or less.

The high-rate X-band downlink at 7 kbps will use a modulation index of 1.4 radians peak, directly modulating the carrier. The mode will use a high-gain antenna of 0.3-m in diameter with about 25.9 dB gain. The system will employ rate 1/6 constraint length 15 convolutional code concatenated with the JPL standard Reed Solomon code. This will provide a bit-error rate of 10^{-6} for a required signal-to-noise ratio of about 0.8 dB. The antenna will have a 3 dB beamwidth of about 6.97°, and, for a loss of 0.1 dB, the pointing accuracy will have to be around 0.65°. The antenna pointing will be done by the ADCS system. It is assumed the DSN receiver will have a bandwidth of about 5 Hz. With this assumption, the data margin will be about 3 dB and the carrier margin will be at least 6 dB. Table 13-1 shows this link budget.

The low-rate (10 bps) mode telecom will use two 0.03-m low-gain patch antennas (LGA), each with a 3-dB beamwidth of about 67.2°. The LGAs will not need pointing. This link will also use the same coding scheme used by the high-rate downlink. Under these conditions the link will provide a reasonable data margin of 3 dB and a carrier margin of about 6 dB. Table 13-2 shows the link budget for this case.

For emergency mode communications that use the low-rate mode, the two antennas will be mounted about 180° from each other around the spacecraft. In case of an emergency with a partial loss of attitude control, the spacecraft will be pointed towards the Sun; and the LGA, with a 3 dB end-to-end beamwidth of about 67.2°, will transmit the spacecraft data to the ground. In the case of total failure of the Attitude Control System, the CDS computer will switch between the antennas in a predetermined way to transmit the emergency mode data generated on board. In both cases the link is a viable link with reasonable margins.

Emergency commanding will be done using the 34-m BWG antenna to transmit X-band at 20 kW. The spacecraft will use the X-band LGA. This link will have reasonable margins.

It should be noted that the telecom will fully comply with the Consultative Committee for Space Data Systems (CCSDS) transfer-frame formats since the DSN will be working on CCSDS formats only. This implies that the bit-error rate assumed for the transfer frame in the link budget, i.e., 10^{-6} will produce a larger bit-error-rate, like 10^{-5} for the data bits.

The telecommunications systems hardware, mass, power consumption, and cost for one spacecraft are presented in Tables 13-4 and 13-5. This cost assumes redundant systems, Class C Mission system integration, Class B parts. The telecommunications subsystem designers

recommend spares for both the antenna and the transponder. The cost includes a spare antenna ($55K), and a spare transponder ($450K).

Table 13-1 Link budget for high-rate downlink.

Link Gains	
Range	0.34 AU
Link Frequency (MHz)	8450.00
Space Loss (dB)	265.11
Earth Station Antenna Name & Diameter	DSN 34BWG
Earth Station Antenna Elevation Angle (deg)	10.0
Earth Station Antenna G/kT (dB/K)	279.60
Total Loss in the Link (dB)	5.00
Data Channel	
Modulation Index (peak radians)	1.40
Subcarrier Modulation	square
Modulation Loss (dB)	0.13
Bit Rate (kbps)	7.0
Bit-Error Rate	1.00E-06
Reed-Solomon Rate	0.17
Constraint Length	15.00
Required Signal-to-Noise Ratio	0.81
Desired Channel 1 Data Margin (dB)	3.00
Carrier Loop Computations	
Carrier Suppression Loss (dB)	15.39
Carrier Loop Bandwidth (Hz)	5.00
Carrier Loop Threshold (dB)	12.00
Desired Carrier Margin (db)	6.00
Transmitter S/C EIRP Calculations for	
Carrier Margin	30.89
Data Channel Margin	32.87
Maximum S/C EIRP Required (dB)	32.87
Transmitted RF Power (W)	5.00
Parabolic Dish Antenna Diameter (m)	0.30
Antenna 3 dB Beamwidth, end-to-end (Deg)	6.97
Ant Eff (%)	55.00
Ant G (dB)	25.88

Table 13-2 Link budget for low-rate downlink.

Link Gains	
Range	0.34 AU
Link Frequency (MHz)	8450.00
Space Loss (dB)	265.11
Earth Station Antenna Name & Diameter	DSN 34BWG
Earth Station Antenna Elevation Angle (deg)	10.0
Earth Station Antenna G/kT (dB/K)	279.60
Total Loss in the Link (dB)	4.00
Data Channel	
Modulation Index (peak radians)	1.00
Subcarrier Modulation	square
Modulation Loss (dB)	1.50
Bit Rate (kbps) (uncoded)	0.01
Bit-Error Rate	1.00E-05
Required Signal-to-Noise Ratio	9.68
Desired Data Margin (dB)	3.00
Carrier Loop Computations	
Carrier Suppression Loss (dB)	5.35
Carrier Loop Expanded BW (Hz)	1.00
Carrier Loop Threshold (dB)	12.00
Desired Carrier Margin (db)	6.00
Transmitter S/C EIRP Calculations for	
Carrier Margin	12.86
Data Channel Margin	13.69
Maximum EIRP Required (dB)	13.69
Transmitted RF Power (W)	5.00
Parabolic Dish Antenna Diameter (m)	0.03
Antenna 3 dB Beamwidth, end-to-end (Deg)	67.22
Ant Eff (%)	55.00
Ant G (dB)	6.70

Table 13-3 Link budget for commanding.

Link Gains	
Range	0.34 AU
Link Frequency (MHz)	8450.00
Space Loss (dB)	265.11
S/C Antenna Diameter	0.03
S/C Antenna G/kT (dB/K)	208.46
Total Loss in the Link (dB)	5.00
Data Channel 1	
Channel Modulation Index (peak radians)	1.50
Subcarrier Modulation	square
Modulation Loss (dB)	0.02
Bit Rate (kbps) (uncoded)	2.00
Bit-Error Rate	1.00E-06
Required Signal-to-Noise Ratio	10.52
Desired Channel 1 Data Margin (dB)	3.00
Carrier Loop Computations	
Carrier Suppression Loss (dB)	23.01
Carrier Loop Expanded BW (Hz)	5.00
Carrier Loop Threshold (dB)	12.00
Desired Carrier Margin (db)	6.00
Transmitter S/C EIRP Calculations for	
Carrier Margin	109.64
Data Channel Margin	108.20
Maximum S/C EIRP Required (dB)	109.64
Transmitted RF Power (W)	20000.00
Parabolic Dish Antenna Diameter (m)	32.69
Antenna 3 dB Beamwidth, end-to-end (Deg)	0.06
Ant Eff (%)	55.00000
Ant G (dB)	66.63

Table 13-4 Hardware, mass, and power for one spacecraft.

Item	Units	Mass (kg)	Power (W)	Notes
HGA	2	1.0		
LGA	4	0.24		
Tiny Transponders	2	1.4	12	
Power Amplifier	2	0.8	15	
Diplexers	1	0.29		
Cables	1 Lot	1.21		
Microwave Components	1 Lot	5		
Totals		9.9	26.4	Science
			12.0	Launch

Table 13-5 Telecommunications cost for one spacecraft.

	Workforce (years)	Costs ($K)		
		Labor	Parts and Contracts	Sub-totals
Antenna Subsystem Engineering	1.0	430	1,500	1,900
Antenna Electrical/RF Design	1.0	150	224	444
Antenna Mechanical Development	0.8	113	1,680	1,845
Telecom Task Management	4.5	900	99	1,089
Telecom Subsystem Engineering	5.0	750	13	1,113
Radio Study	0.2	40	0	40
Product Assurance	0.6	116	0	116
RFS Subsystem Engineering	3.5	520	427	1,198
Microwave Components	1.0	150	207	427
RFS ATLO Support	3.3	500	0	733
SSPA Procurement/Development	0.5	75	1,165	1,275
Tests and System Engineering	0.5	75	2,856	2,966
Telecom Totals	21.8	3,818	8,171	13,145

SECTION 14—GROUND SYSTEMS AND MISSION OPERATIONS

The data collection strategy is summarized in Table 14-1. Two downlink strategies were considered using the 30-cm steerable antenna. One strategy downlinked once every 2 days and a second downlinked once per week. The science team selected the "one downlink every 2 days" option because of the expected savings in spacecraft power requirements. Therefore, Team X recommends carrying 7 kbps for downlink capacity and 70 Mbits for onboard storage of engineering and science data. The data return strategy will be to downlink once per two days in a 10.5-hour time frame, (or equivalent), in the form of

Acquire spacecraft 1	30 min.
Downlink data from spacecraft 1	3 h
Acquire spacecraft 2	30 min.
Downlink data from spacecraft 2	3 h
Acquire spacecraft 3	30 min.
Downlink data from spacecraft 3	3 h

We should note that if the 100 bps of S/C engineering data is not sufficient, the science team may downlink daily and increase the engineering rate to 400 bps with no change in the configuration of the system.

Figure 14-1 shows a ground system layout for the LISA mission. Station support will be through the DSN, and so accordingly, several software subsystems are best taken directly from the DSN Missions Ground Support Operations (MGSO), and adapted for the LISA mission. All navigation functions with the exception of maneuver design will be done by the multi-mission navigation services.

Some or all of the personnel from spacecraft design, development, integration, and test will become part of the operations team. Command and telemetry software developed for operations will be used for support in assembly, test, and launch operations.

The development team and the flight team are modeled after the generic Team X low-cost operations design. We should note that the flight team described here is a critical-mass estimate. There are no provisions for illness, vacations, or transfers taken into account in these numbers.

This estimate assumes the existence of certain services from the Telecommunications and Mission Operations Directorate (TMOD). The project is urged to level requirements on TMOD for these services.

The development cost estimate for mission operations is given in Table 14-2, with the operations cost estimate given in Table 14-3. Each workyear is costed at $200K. This should be sufficient funds to pay for salary, burden, travel, computing resources, and some consulting from the engineer's home section, should it be necessary.

Table 14-1 Operational Guidelines.

MISSION PHASE					Cruise 13 months	Science 3 years
Data Acquisition Scheme	Instantaneous Data Rate	Unit	Compression Rate between Instrument & CDS	Compression Rate between CDS & Telecom		
Laser 1 & 2	1000.0	bps	1	5	no science in cruise	takes data continuously
Inst. Engineering Data	100.0	bps				
S/C Engineering Data	100.0	bps				
				100% data return required?	No, degrades gracefully	
				Minimum time to data being returned?	No hard constraint	
				Adaptive commanding?	No	

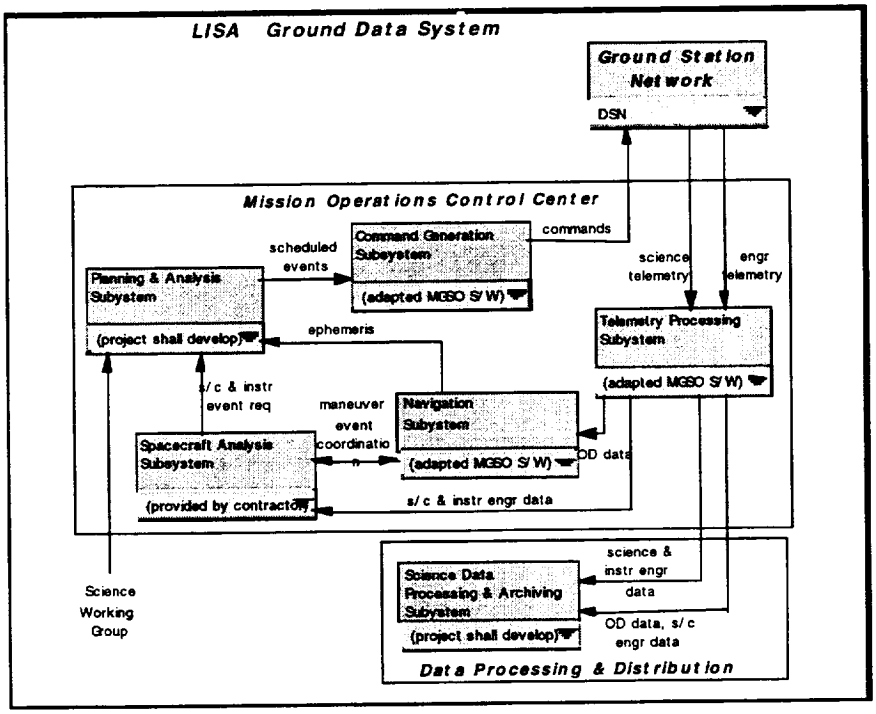

Figure 14-1 LISA ground data system.

Table 14-2 Ground system development cost estimate.

1.7 GROUND SYSTEM DEVELOPMENT	Annual Staffing	Annual Project External Resources		Total Workyear Equivalents	Total Cost ($/K)
1.7.1 Mission Operations Plan				2.5	500.0
Traj design	0				
Data collection scenario	0.5				
DSN prelaunch schedule	0.5				
1.7.2 Ground Software Development				20.0	4000.0
Planning & Analysis Subsystem	3				
Command Generation Subsystem	0.5		0.5		
Telemetry Processing Subsystem	0.5		0.5		
Spacecraft Analysis Subsystem	0				
Navigation Subsystem	0		3		
Command Simulator	0				
1.7.3 Data Processing				11.3	2250.0
Level 0 Processing S/W & Proc.	0		1		
Levels 1-n Processing S/W & Proc.	0		3		
Data Archiving S/W & Proc	0		0.5		
1.7.4 Ops Management & Infrastructure				7.5	1500.0
Ops Development Manager	1				
Computer System Manager	1				
EEIS/MOS Engineer	1				
1.7.5 L + 30 Days				2.0	400.0
				43.3	8650.0
Years of Development					

Table 14-3 Mission operations cost estimate.

1.7 MISSION OPERATIONS	Annual Staffing	Annual Project External Resources		Total Workyear Equivalents	Total Cost ($/K)
1.7.6 Flight System Operations				29.6	5920.0
Mission Director	1				
Mission Planning/DSN	1				
Navigation	1				
S/C Engineering	3				
Instrument Engineering	1				
Data Archiving	0		0.25		
Command Simulator Ops	0				
1.7.7 Tracking, Data Acquisition, & Institutional Support				49.3	9866.4
Multi-mission Ops Support	0		0.5		
Antenna Support			1916.25		
Multi-mission NAV	0		2		
1.7.3 Data Processing				9.2	1837.5
Level 0 Processing & Data Dist.	0		1		
Levels 1-n Processing	0		1		
Data Archiving	0		0.25		
1.7.4 Ops Management & Infrastructure				18.2	3634.2
Project Manager	1				
Secretary	1				
PIO	0.2		0		
Budget AA	1				
MGSO Config & Adapt. (CAT) Team			0.25		
Computer System Administrator	1				
				106.3	21258.0
Years of Ops					

SECTION 15—COST

15.1 INTRODUCTION

Baseline project costs were estimated by Team X for the Laser Interferometer Space Antenna (LISA) Mission. This mission consists of three spacecraft launched on a single launch vehicle. The science module together with a propulsion module constitutes one spacecraft, so there are three of these combinations. After separation from the launch vehicle, the three stacked "sciencecraft" separate into three and are placed individually by their propulsion modules into a science orbit at 1 AU (150×10^6 km). The mission duration was specified as a 13-month cruise to the science orbit followed by 3 years of science observations. An additional 7-year extended mission (for a total of 10 years) was a goal but was not to drive the design or the cost.

It is expected that the European Space Agency (ESA) will be providing some of the hardware for the LISA mission, such as the inertial sensors, the lasers, and the FEEPs. Their total contribution should offset about $50M of total project cost.

The cost guidelines for this mission are given in Table 15-1. These guidelines include a $300M NASA cost goal. The ESA contribution of $50M is over and above this goal. This mission has selected, high redundancy along with selected spares. It would be launched in 2004 on a Delta 7925H launch vehicle, it would have 4.1 years of mission operations. The design and development phase would be 30 months. This astrophysics mission is a specialized mission and is more characteristic of a deep space project than a near-Earth lite-sat. Its payload consists of the three spacecraft that each contain inertial sensors, lasers, and small telescopes. Team X used its Deep Space Cost Model to estimate the costs for this project. Aware that this is not a full deep-space mission, and that it included three identical spacecraft, reserves were set at 17% instead of the usual 20%.

The cost model for the LISA Mission includes

- Quasi-grass roots cost estimates for the spacecraft subsystems, mission operations, science team, and launch vehicle.
- Historical cost models for the various other mission components including payload, systems engineering, integration and test/ATLO, project office, outreach, phase A, phase B, and reserves.

15.2 COST RESULTS

The estimated subsystem costs (for the solar-electric propulsion option) are given in Table 15-2. The estimated project costs are shown in Tables 15-3 and 15-4 based on the inputs given in Table 15-1 and on the discussions held with Team X. (A more detailed breakdown is given in the cost model computer runs.) These costs cover the entire mission and include all mission elements, launch vehicle, all phases, and reserves. It must be remembered that this mission involves three spacecraft on one launch vehicle so that the individual subsystem costs each reflect three sets of flight hardware. The total cost without launch vehicle and reserves is $348M. If LISA could be launched on the Delta 7925 instead of the 7925H, its cost could decrease by about $6M.

Table 15-1 LISA cost guidelines.

Mission Parameter	Description
Trajectory	Sun elliptical, 1-AU (150×10^6 km), 20° (52×10^6 km) behind Earth
Science/instruments	3 sciencecraft, each with inertial sensors/test mass, 1-W laser ranging with two 30-cm telescopes
Desired launch vehicle	Delta 7925H
Assumed launch date	July 2004
Cost target	$300M - US contribution
Hardware	3 flight S/C plus 1 partial prototype/breadboard instrument
FY $ (year)	1997
Phase A start date	July, 1999
Phase A duration	12 months
Phase B duration	18 months
Phase C/D duration	30 months
Phase E duration	49 months
Redundancy	Selected - high
Spares approach	Selected
Stabilization	3-axis
Parts class	Commercial & Class B
S/C supplier	Industry—custom
Instrument supplier	University of Colorado & ESA
I&T site	S/C contractor
Burdens—JPL program office	Space and Earth Science
L/V capability	C3 = 1+, 1400 kg
P/L mass estimate	210 kg (for all three spacecraft)
Radiation total dose	2.7 krad/year; 11-krad baseline
Post-launch delta-V	1350 m/s worst case
Reserves	17%

Table 15-2 Subsystem cost for solar-electric propulsion.

Subsystem	Design	Test	Test H/W	FLT H/W 1 unit	EM + Spares	FLT H/W all units	Subsystem Total $M
Structures, Mechanisms	4.50	0.50	0.50	4.30	0.25	11.61	17.11
Prop Module Structure	4.60	0.60	0.50	4.90	0.30	13.23	18.93
Power Source-chem/SEP	1.10	2.80	0.38	4.20	0.35	12.60	16.88
Computer H/W	2.04	2.10	0.25		1.40	4.98	9.37
Software	1.23	0.45	0.30			0.60	2.58
Attitude Control	4.59	9.38	1.96	8.32	1.75	20.81	36.74
Telecommunications	3.94	2.63	0.00	6.57	1.97	18.33	24.90
Propulsion-chem	1.60	1.10	0.00	1.30	0.20	6.90	9.60
Propulsion-SEP	1.60	1.10	0.00	4.10	1.20	12.60	15.30
FEEPs	1.32	1.32	0.70	2.23		6.68	10.02
Thermal	0.26	0.18	0.00	0.63	0.10	1.00	1.44
Spacecraft Total, $M	26.79	22.15	4.59	36.55	7.52	109.34	162.87
Science Instruments (S/C)	8.88	5.92	0.00	18.50	2.00	43.30	58.10

Table 15-3 Phase C/D cost for solar-electric propulsion.

Element	Cost ($M)
Project Office	11
Outreach	3
Mission Analysis and Engineering	3
Payload	58
Spacecraft	163
ATLO/I&T	40
Science Team	3
Mission Operations	9
Total	289

Table 15-4 LISA total project cost for solar-electric propulsion.

Element	Cost ($M)
Phase A: Conception	6
Phase B: Preliminary Design	20
Phase C/D Design/Development	289
Phase E: Mission Operations	33
Reserves	59
Launch Vehicle	59
Total	465
ESA Component	50
NASA Component	415

The biggest cost driver is the science instruments at $58M which includes three sets of thermal shields, telescope assemblies, electronics, and laser assemblies. Other big cost drivers are attitude control ($37M), propulsion ($25M), telecommunications ($25M), and ATLO/I&T ($38M). The attitude control subsystem will be adapted and customized from a commercial bus. It will also need to provide attitude/translation sensing, determination, and control in the nanoradian/nanometer range. Propulsion will be done with xenon-ion thrusters, with monopropellant thrusters for attitude control. Telecommunications will use X-band transmission. It will also use two high-gain antennas and four low-gain antennas. The ATLO/I&T fraction of total hardware cost is reduced for the production of multiple units (three in this case) so that it represents 18% of the total of the hardware subsystem costs. Figure 15-1 shows a typical cost expenditure profiles for the LISA Mission given the programmatic guidelines of Table 15-1.

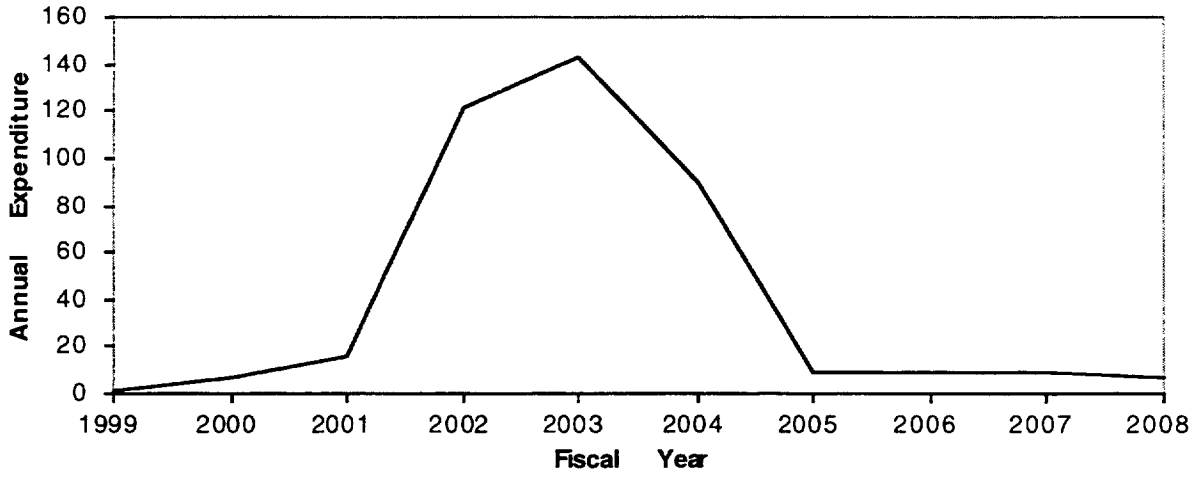

Figure 15-1 Typical cost expenditure profile.

SECTION 16—CHEMICAL PROPULSION OPTION

16.1 INTRODUCTION

A chemical propulsion option was also considered by Team-X. The differences between the solar electric propulsion (SEP) option and the chemical option are given in this section. It became apparent in the study that the chemical propellant option would not fit within the constraints of a Delta-II launch vehicle, being considerably over the mass limit. Because of this, the study of the chemical propellant option was not completed, particularly in regard to the Structure. However, it appeared that the spacecraft cost would be lower with the chemical propellant option. If the cost of a Delta-III, with its much greater mass capability, was not too much higher than the baseline Delta-II 7925H, then the chemical propellant option might end up being less expensive overall.

The chemical option differs from the SEP option primarily in the propulsion subsystem. The power subsystem is substantially the same except for eliminating the deployed solar arrays for the ion engine. The elimination of these arrays also removes the need in the attitude control subsystem for a mechanism to control the array pointing, and in the structure for the deployment mechanism.

16.2 SYSTEMS ENGINEERING

A bipropellant system is required for the chemical propulsion option because of the mass limitation and the ΔV requirement of 1050 m/s per spacecraft. The propellant mass shown in Table 16-1 is for the spacecraft mass that would be required to fit this mission on a Delta 7925H launch vehicle. Unfortunately, the mass estimated during the study was considerable larger than the Delta can accommodate. The propellant mass was not adjusted upward since the design was not feasible on the desired vehicle.

Performance estimates for the Delta III lie between 2600 kg and 2700 kg for launch C3s between 1 km^2/s^2 and 2 km^2/s^2. These data are from the McDonnell Douglas *Delta III Payload Planners Guide* of April 1996, and a launch contingency of 10% is the minimum that should be considered. This performance is for the two-stage Delta III (with no PAM-D third stage); at these low launch energies, the STAR 48 used in the PAM-D third stage does not add any mass performance at all. (That is not true for the Delta II—the 7925 injects significantly more mass than the 7920 at all planetary launch energies.)

16.3 PROPULSION

The chemical propulsion module uses dual-mode technology for the best total system performance. Dimensional constraints of 40-cm height and 1.8-m diameter imposed on the propulsion module forced the system to have multiple main engines and propellant tanks, penalizing the mass and cost of the system compared to an optimum configuration.

Table 16-1 Systems summary.

	Mass (kg)	Mode 1 Power (W)	Mode 2 Power (W)	Mode 3 Power (W)		NASA TRL
ScienceCraft (ea.)		*Science xmit on*	*Propulsion Module*	*Launch*		
Payload						
Instruments	70.0	72.2	0.0	0.0		5
Thermal Tube	14.2	0.0				
Payload Total	84.2	72.2	0.0	0.0		
Bus						
Attitude Control	6.0	2.1	11.7	12.2		5
Command & Data	14.5	13.1	13.1	13.1		6
Power	12.2	13.7	8.3	11.6		5
Structure	41.1	0.0	0.0	0.0		6
Cabling	15.4					
Propulsion (FEEPs incl. Drivers)	18.0	22.0	N/A	N/A		5
Telecomm	5.2	18.4	4.0	18.6		5
Thermal	1.7	0.0	17.0	17.0		7
Bus Total	114.1	69.3	54.0	72.4		
ScienceCraft Total (Dry)	198.3	141.5	54.0	72.4		
Mass/Power Contingency	59.5	42.4	16.2	21.7		
ScienceCraft with Contingency (ea.)	**257.8**	**183.9**	**115.5**	**152.8**		
			Incl. Prop. Module			
Propulsion Module (ea.)						
Structure/Mechanisms	53.0	N/A				
Thermal	3.0	N/A	17.0	17.0		
Propulsion	56.1	N/A	17.8	28.1		6
Cabling	5.0	N/A				
Prop Module Total (Dry)	117.1	N/A	34.8	45.1		
Mass/Power Contingency	35.1	N/A	10.4	13.5		
Dry Prop Module w/Contingency	**152.2**	**N/A**	**45.2**	**58.6**		
Propellant & Pressurant	152.6	Propellant based on S/C mass =455				
Wet Prop Module with/Contingency (ea.)	**304.8**					
Total for 3 Sciencecraft/Prop Module	**1687.9**					
S/C Adapter	26.6	w/30% contingency				
L/V Adapter *Delta supplies*	0.0	w/10% contingency				
Launch Mass	**1714.5**					
Launch Vehicle Capability	1391.2	Delta 7925-H		1.115	Launch C_3	9
Launch Vehicle Margin	**-323.3**		**-23.2%**			

Contingencies		
	Mass	Power
Instruments	30%	30%
Other	N/A	N/A
S/C, dry	30%	30%

Stabilization: cruise	**3-axis**	Pointing Direction: cruise	**Sun**
Stabilization: science	**3-axis**	Pointing Direction: science	**Inertial**
Radiation Total Dose, krad	**11 krad**	Mission Duration	**4.1 year**
Bit-Error Rate	1.00E-05	Instrument Data Rate	**200 bps** compressed
Redundancy	**High**	Data Storage	**8 Mbytes**

The chemical propulsion module is a pressure-regulated dual-mode system utilizing N_2O_4 and hydrazine (N_2H_4) propellants in the main propulsion bipropellant mode, and the N_2H_4 for monopropellant functions. The module height limit forces the use of multiple engines for the main propulsion function, since the applicable engines that could provide the thrust in a single unit are approximately 65 cm long. The Royal Ordnance Leros 20H engine was selected. This engine is in development with potential application in communication satellites. It provides a 22-N thrust at a 0.8 oxidizer-to-fuel mixture ratio and is projected to deliver 300-s specific impulse. Four Leros 20H engines are used for the main velocity increment functions. The engines are mounted in pairs 180° apart. In the event of malfunction of one engine, the opposite unit

would be shut down and the remaining pair of engines would complete the mission. This arrangement provides redundancy for the ΔV functions without upsetting attitude control capability. Monopropellant thruster functions of small velocity increments and reaction control torques are provided by four Primex Technologies Model MR-111C thrusters at 4.45-N thrust, and four Primex Model MR-103C thrusters at 0.9-N thrust. The high-thrust monopropellant thrusters fire in the same axes as the main engines, and the low-thrust units are mounted to provide couples for roll control.

Multiple propellant and pressurant tanks are also required to carry the propellants and remain within the module height limit. The propellants required were calculated assuming the launch mass of the spacecraft system would be 475 kg, and the total velocity increment required would be 1050 m/s. In addition, 5 kg of N_2H_4 was carried for the attitude-control requirements. An existing tank design by Pressure Systems, Inc. was assumed. The same design, model 80213-1, can be used for both propellants. The tank is a spherical design of 6Al-4V titanium and has a surface tension propellant management device. Three of these tanks are required to hold the N_2O_4, and five are required to hold the N_2O_4. Two tanks are required to hold the He pressurant. These tanks are also an existing Pressure Systems, Inc. design (model 80345-1). The mission profile has long-duration coasting between main-engine firings. This requires the pressure control and propellant isolation subsystems of the propulsion system to have the capability to open, isolate, and reopen certain segments to protect against leakage and detrimental effects from the N_2O_4 oxidizer during the coast periods. These subsystems were therefore based on the related Mars Global Surveyor propulsion system design.

The mass of the propulsion system is broken down in Table 16-2.

Table 16-2 Chemical propulsion subsystem mass.

Element	Mass (kg)
Main Engines: four Leros 20H	3.4
Thrusters: four MR111C & four MR103C	3.2
Pressure Control System	29.2
Propellant Tanks, eight	14.5
Pressurant Tanks, two	6.7
N_2O_4	65.3
N_2H_4	86.6
He	0.7
Total Loaded Mass	208.7

The cost for this system is estimated to total $30.5M for the three modules required. The cost breakdown is $3.2M for design, analyses, procurement engineering, and management of the first system and $0.7M for these functions for each of the next two systems: $4.0M for fabrication, assembly, and test of the propulsion system and subsystem support to ATLO for the first system, and $3.6M for these functions for each of the next two systems: $5.7M for procurements for the first system, including $0.7M for spares applicable to the complete program, and $4.5M for procurements for each of the next two systems.

16.4 STRUCTURES

The total available height in the launch fairing limits the height of each of the propulsion modules to 40 cm. This, in turn, forces the propellant to be stored in eight separate tanks of

34-cm diameter plus two helium pressurant tanks of 24-cm diameter, each of which, with the four engines and propellant management hardware, has to be mounted by the propulsion module structure.

Conceptually, the propulsion module is fairly simple since it contains only the propulsion hardware (10 tanks, 4 engines, and flow control hardware) and necessary thermal equipment and cabling. As with the sciencecraft module, the propulsion module also needs additional pass-through cabling, connectors, and wiring separation devices for as many as (in the case of the "bottom" module) four separate stacked modules, which were not considered in the cabling estimate in the table below.

Each propulsion module carries two separation systems, so that the sciencecraft will not be burdened with them. The mass of the separation system needs to be better defined in future work, due to the science team's choice to drop the clamp-band separation system in favor of explosive bolts, given the large mass of the clamp-band system. The mass breakdown for the propulsion module structure is given in Table 16-3.

Table 16-3 Propulsion module structure mass.

Element	Mass
Outer cylinder, 40 cm high, 1.8-m diameter, 2-mm wall	7.5
Top/bottom plates, 1.6 mm, 1.8-m diameter (2)	16.
Interface rings, scaled from ESA estimate (2)	11.
Joints, fittings	6.
Separation system (2)	4.
Separation pyros	2.
Interface hardware & misc.	3.
Balance mass	3.
Cabling	5.
Total (less LV adapters)	58.

The propulsion module structure costs given in Table 16-4 are lower for the chemical-propellant version because of need of the SEP option for additional solar-array structure, outriggers and latch/deploy mechanisms, and the engine gimbal mechanisms (which are bookkept on the antenna-articulation-mechanism line).

Table 16-4 Chemical propulsion module structure cost ($M).

	Total	Non-R.	Recurr.	Design	Dev. Test	Qual. Test	Flt. H/W
Bus Structure	2.80	1.60	1.20	1.50	0.10	0.10	1.10
Solar Array Structure	0.60	0.30	0.30	0.30			0.30
Separation Mech.	1.40	0.50	0.90	0.40	0.10	0.10	0.80
Integration Hardware & AHSE	0.50	0.30	0.20	0.20	0.10		0.20
Misc.	0.60	0.30	0.30	0.20	0.10	0.05	0.25
Adapter, Spacecraft side	0.30	0.20	0.10	0.20			0.10
Cabling	0.70	0.40	0.30	0.40		0.05	0.25
Total	6.90	3.60	3.30	3.20	0.40	0.30	3.00

16.5 ATTITUDE DETERMINATION AND CONTROL SYSTEM

The main difference from the SEP option for the ADCS with the chemical propulsion option is that articulation of the SEP solar panels is no longer needed. A redundant pair of propulsion valve drive electronics placed on MCMs will allow the spacecraft CDS computer to control the hydrazine thrusters and four bipropellant engines.

Table 16-5 gives a mass and power estimate summary of the ADCS subsystem for the chemical propulsion option, and Figure 16-1 is a functional block diagram of the ADCS. Table 16-6 gives a cost breakdown for this subsystem for one spacecraft.

Table 16-5 ADCS hardware components for chemical propulsion option.

	Unit	Mass [kg]	Power (W)				Comments
			Max	Science	Cruise	Launch	
Fine Sun Sensors	2	1.28	0.50	0.50	0.50	0.50	128° × 128° FOV 0.002° accuracy Commercial heritage.
Star Cameras	4	2.00	1.00	1.00	0.50	1.00	2-arcsec pitch & yaw. 16-arcsec boresight roll. Ørsted/Pluto Express heritage.
Inertial Reference Units	2	1.40	10.00	0.00	10.00	10.00	Fiber-optic gyros. 0.2°/hr bias stability. Clementine/DS-1 heritage.
Coarse Sun Sensors	10	0.10	0.00	0.00	0.00	0.00	Simple Silicon photodiodes to provide 4-p steradian coarse coverage.
Interface Electronics	2	0.20	0.10	0.10	0.10	0.10	MCM. DS-1/2/3 heritage.
Propulsion Valve Drive Electronics	2	0.20	0.10	0.00	0.10	0.10	Valve drivers for Propulsion Module. MCM. DS-1/Pluto Express heritage.
HGA Antenna Drive Electronics	2	0.80	0.50	0.50	0.50	0.50	MCM. DS-1/2/3 heritage.
Shielding		0.00					
TOTAL	26	5.98	12.20	2.10	11.70	12.20	

Table 16-6 ADCS cost estimate for chemical propulsion option.

Component	Cost (FY97 $K)
System Engineering	656
Controls and Analysis	1,636
Software	2,406
Integration and Test	6,223
Ground System Engineering	1,910
H/W Engineering	2,599
Flight Hardware	6,022
Flight Spares and EMs	1,477
Total	22,927

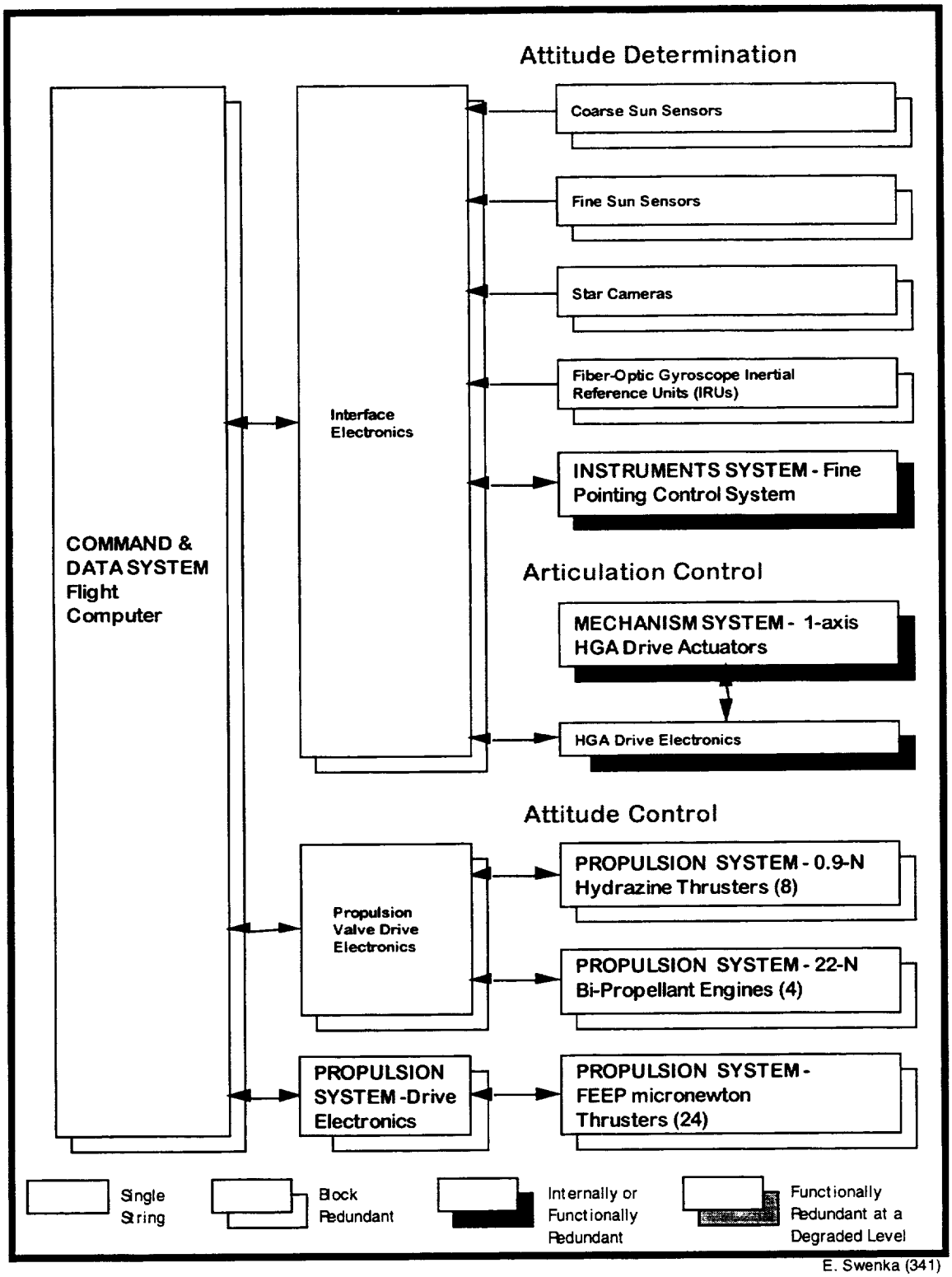

Figure 16-1 ADCS functional block diagram for chemical propulsion option.

16.6 COST COMPARISON

The subsystems costs for the chemical propulsion option are given in Table 16-7. The estimated project costs are shown in Tables 16-8 and 16-9. The chemical propulsion option cost is $443M (FY'97$). This is $22M lower than for the SEP option, because of reduced costs from eliminating the power needs of the ion engine (reflected in the Power, ADCS, and Structures subsystems), which are partly offset by higher propulsion system costs for the multiple tanks and thrusters. In addition the Mission Operations cost estimate is slightly smaller since only a few discrete maneuvers would be needed, which is expected to require less monitoring than the nearly continuous thrusting in the SEP option.

The biggest cost driver is still the science instruments at $58M, which includes three sets of thermal shields, telescope assemblies, electronics, and laser assemblies. Other big cost drivers are attitude control ($34M), propulsion ($31M), telecommunications ($25M), and ATLO/I&T ($36M).

This lower cost estimate does not take into account that the system as designed cannot be launched by the selected launch vehicle. If the cost of a Delta-III were included instead, the cost would be higher than for the SEP option.

Table 16-7 Subsystem costs for chemical propulsion option.

Subsystem	Design	Test	Test H/W	FLT H/W unit 1	FLT H/W all units	EM + Spares	Total Subsystem Cost
Structures, Mechanisms	4.50	0.50	0.50	4.30	11.61	0.25	17.11
Prop Module Structure	2.90	0.40	0.30	2.40	6.48	0.30	10.08
Power Source	0.90	1.90	0.25	2.91	8.72	0.35	11.77
Computer Hardware	2.54	1.35	0.35		4.97	1.40	9.21
Software	1.20	0.60	0.15		0.60		2.55
Attitude Control	4.47	9.05	1.91	7.50	18.75	1.48	34.18
Telecommunications	3.90	2.60	0.00	6.60	18.40	1.98	24.90
Propulsion	3.20	4.00	0.00	5.70	23.30	0.70	30.50
FEEPs	1.32	1.32	0.70	2.23	6.68	0.30	10.02
Thermal	0.26	0.18	0.00	0.63	1.00	0.10	1.44
Spacecraft Total	25.19	21.89	4.16	32.26	100.51	6.86	151.76
Science Instruments	8.88	5.92	0.00	18.50	43.30	2.00	58.10

Table 16-8 Phase C/D cost with chemical propellant option.

Element	Cost ($M)
Project office	10
Outreach	3
MA&E	2
Payload	58
Spacecraft	151
ATLO/I&T	38
Science team	3
Mission operations	8
Total	273

Table 16-9 LISA total project cost with chemical propulsion.

Element	Cost ($M)
Phase A: Conception	5
Phase B: Preliminary design	19
Phase C/D Design/development	270
Phase E: MO&DA	32
Reserves	56
Launch vehicle	59
Total	441
ESA component	50
NASA component	391

SECTION 17—ISSUES AND CONCERNS

17.1 INSTRUMENT COST

The largest cost element in the study was that of the science instruments. This cost is also the most poorly defined. The cost estimate was made using a simple model based on the instrument mass.

17.2 STRUCTURAL DESIGN AND COST

There was insufficient time during the study to assess the structural design. A preliminary analysis had been done before the study to show that the basic configuration was feasible. However this was based on the assumption of a clamp-band separation system. It was discovered during the study that mass needed for the clamp-band system was larger than had been thought so it might be preferable to use explosive bolts for separation. While this option was used in the mass and cost estimates, more work is needed to see if enough mass has been allocated for the explosive-bolt attachment points.

17.3 MISSION DESIGN

The modeled cost for Mission Analysis and Engineering is half the normal percentage of the Phase C/D costs. This covers trajectory design, mission plan, navigation plan, mission requirements, launch planning, etc., for both the transfer trajectory and the operations orbit. The science team argued that, with no planned maneuvers after reaching the operational orbit and no planned pointing activities other than the slow one-per-year revolution, there would be much less work involved than a normal planetary mission. The study leader expressed reservations about this assumption.

17.4 PROPULSION

The study leader felt that the configuration of the attitude control thrusters on the SEP Module should be given further consideration. The arrangement required for aiming the thrust vector of the SEP thrusters may require addition of more N_2H_4 thrusters than assumed here to provide three-axis control for both SEP operations and operation of the N_2H_4 system for separation, etc.

SECTION 18—REFERENCES

A. Abramovici et al., *Science*, Vol. 256, 325–333 (1992).

T. A. Apostolatos et al., *Phys. Rev. D*, Vol. 49, 6274 (1994).

G. Bradaschia et al., *Nucl. Instrum. and Methods A*, Vol. 289, 518 (1990).

A. Chokshi and E. L. Turner, *MNRAS*, Vol. 259, 421 (1992).

C. Cutler et al., *Phys. Rev. Let.*, Vol. 70, 2984 (1993).

C. Cutler and E. Flanagan, *Phys. Rev. D*, Vol. 49, 2658 (1994).

K. Danzmann et al., Lecture Notes in *Physics*, Vol. 410, 184–266, Springer, Heidelberg (1992).

L. P. David, R. H. Durisen, and H. N. Cohn, *Astrophys. J.*, Vol. 316, 505 (1987).

Delta III Payload Planners Guide, Report MDC 95H0137A, Boeing Co. (Huntington Beach, CA), (March 1997).

M. J. Duncan and S. L. Shapiro, *Astrophys. J.*, Vol. 268, 565 (1983).

D. J. Eisenstein and A. Loeb, *Astrophys. J.*, Vol. 443, 11 (1995).

C. R. Evans, I. Iben, and L. Smarr, *Astrophys. J.*, Vol. 323, 129 (1987).

A. E. Evrard, in "The Environment and Evolution of Galaxies," (eds J. M. Shull and H. A. Thronson, Kluwer Acad. Pub.), p. 69 (1994).

W. M. Folkner et al., Proceedings of the Seventh Marcel Grossman Meeting on General Relativity, (1994).

H. C. Ford et al., *Astrophys. J.*, Vol. 435, L27–30 (1994).

G. Giampieri, R. W. Hellings, M. Tinto, and J. E. Faller, *Optics Communications*, Vol. 123, 669–678 (1996).

M. G. Haehnelt, *MNRAS*, Vol. 269, 199 (1994).

M. G. Haehnelt and M. J. Rees, *MNRAS*, Vol. 263, 168 (1993).

R. J. Harms et al., *Astrophys. J.*, Vol. 435, L35–38 (1994).

L. Hernquist, in "The Environment and Evolution of Galaxies," (eds. J. M. Shull and H. A. Thronson, Kluwer Acad. Pub.), p. 327 (1994).

D. Hils and P. L. Bender, *Astrophys. J.*, Vol. L7 (1997).

D. Hils, P. L. Bender, and R. F. Webbink, *Astrophys. J.*, Vol. 360, 75 (1990).

J. Hough et al., "Proposal for a Joint German-British Gravitational Wave Detector," Max-Planck-Institut für Quantenoptik, Report No. MPQ 147 (1989).

I. Iben and A. V. Tutukov, *Astrophys. J. Sup.*, Vol. 54, 335 (1984).

T. R. Lauer et al., *Astron. J.*, Vol. 104, 552 (1992).

T. R. Lauer et al., *Astron. J.*, Vol. 106, 1436 (1993).

B. W. Murphy, H. N. Cohn, and R. H. Durisen, *Astrophys. J.*, Vol. 370, 60 (1989).

R. Narayan, T. Piran, and A. Shemi, *Astrophys. J.*, Vol. 379, L 17 (1991).

E. S. Phinney, *Astrophys. J.*, Vol. 380, L 17 (1991).

G. D. Quinlan and S. L. Shapiro, *Astrophys J.*, Vol. 356, 483 (1990).

M. J. Rees, *Class. Quantum Grav.*, Vol. 14, 1411 (1997a).

M. J. Rees, "Black Holes in Galactic Nuclei," in *Reviews in Modern Astron.*, Vol. 10, 179 (1997b).

E. L. Robinson and A. W. Shafter, *Astrophys. J.*, Vol. 332, 296 (1987).

N. Roos, *Astron. Astrophys.*, Vol. 104, 218 (1981).

N. Roos, *Astrophys. J.*, Vol. 294, 479 (1985a).

N. Roos, *Astrophys. J.*, Vol. 294, 486 (1985b).

S. Sigurdsson, *Class. Quantum Grav.* Vol. 14, 1425 (1997).

S. Sigurdsson and M. J. Rees, *MNRAS* Vol. 284, 318 (1997).

A. Soltan, *MNRAS*, Vol. 200, 115 (1982).

J. H. Taylor and J. M. Weisberg, *Astrophys. J.*, Vol. 345, 434-450 (1989).

A. Toomre, in "The Evolution of Galaxies and Stellar Populations," (eds. B. M. Tinsley and R. B. Larson, Yale Univ. Obs.) p. 401 (1977).

A. V. Tutukov and L. R. Yungelson, *Sov. Astr.*, Vol. 30, 598 (1986).

A. V. Tutukov and L. R. Yungelson, *MNRAS*, Vol. 260, 675 (1993).

M. Umemura, A. Loeb, and E. L. Turner, *Astrophys. J.*, Vol. 419, 459–468 (1993).

R. F. Webbink, *Astrophys. J.*, Vol. 277, 355 (1984).

H. Yamaoka, T. Shigeyama, and K. Nomoto, *Astron. Astrophys.*, Vol. 267, 433 (1993).

ACRONYM LIST

A/D	analog-to-digital converter
AA	administrative assistant
ADCS	Attitude Determination and Control System
Ahr	ampere-hour
ATLO	assembly, test, and launch operations
AU	astronomical unit (Sun-to-Earth distance, 150×10^6 km)
BH	black hole
bps	bits per second
BWG	beam waveguide
C_3	normalized excess launch energy
CAT	Configuration and Adaption Team
CCD	charged-couple device
CCSDS	Consultative Committee for Space Data Systems
CDS	Command and Data System
COBE	Cosmic Background Explorer
CPU	central processing unit
CWDB	close white dwarf binaries
DRAM	Dynamic Random Access Memory
DS-1	Deep Space-1
DSN	Deep Space Network
EEIS/MOS	end-to-end information system/mission operations system
EEPROM	electrically erasable-programmable read-only memory
EIRP	equivalent isotropic radiated power
EM	engineering model
ESA	European Space Agency
ESOC	European Space Operations Center
FEEP	field-emission electric propulsion
FOV	field-of-view
FPGA	field programmable gate array
FSW	flight software
FY	fiscal year
GDS	Ground Data System
GSFC	Goddard Space Flight Center
HGA	high-gain antenna
HST	Hubble Space Telescope
I&T	integration and test
I/F	interface
I/O	input/output
IEEE	Institute of Electrical and Electronics Engineers
IRU	inertial reference unit
JILA	Joint Institute Laboratory for Astrophysics
JPL	Jet Propulsion Laboratory
Kbits	kilobits (thousand, 10^3)
L/V	launch vehicle
LGA	low-gain antenna
LISA	Laser Interferometer Space Antenna
MBH	massive black hole

Mbits	megabits (million, 10^6)
MCM	multi-chip module
MGSO	Mission Ground Support Operations (at JPL)
Mips	million instructions per second
MO&DA	mission operations and data analysis
$M_\odot$	solar mass, 1.99×10^{30} kg
N_2H_4	hydrazine
N_2O_4	nitrogen tetroxide
NPO	numerically programmed
NS	neutron star
P/L	payload
pc	parsec, 3×10^{13} km
PCU	Power Control Unit
PIO	Public Information Office (at JPL)
PPU	Power Processing Unit
PROM	Programmable Read-Only Memory
PSI	Pressure Systems, Inc.
QML	Qualified Manufacturers List
RAM	random access memory
RDM	radiation design margin
RFI	Request For Interest
RFS	Radio Frequency System
rms	root mean square
ROM	read-only memory
S/A	solar array
S/C	Spacecraft
SDST	small deep space transponder
SE	Support Equipment
SECDED	single error correction double error detection
SEP	solar-electric propulsion
SRAM	static random access memory
SSAC	Space Science Advisory Committee
T&I	test and integration
TID	total ionizing dose
TMOD	Telecommunications and Mission Operations Directorate (at JPL)
TRL	Technology Readiness Level (NASA)
ULE	ultralow expansion
USO	ultrastable oscillator
VME	Versa Module Eurocard
WD	white dwarf
WD-WD	white dwarf binary
X-Band	7.2-GHz uplink, 8.4-GHz downlink
YAG	yittrium-aluminum-garnet

REPORT DOCUMENTATION PAGE

Form Approved
OMB No. 0704-0188

1. AGENCY USE ONLY *(Leave blank)*	2. REPORT DATE	3. REPORT TYPE AND DATES COVERED
	03/02/98	Final

4. TITLE AND SUBTITLE
LISA Mission Concept Sudy, Laser Interferometer Space Antenna for the Detection and Observation of Gravitational Waves

5. FUNDING NUMBERS
C - NAS7-1260
B05510021096

6. AUTHOR(S)
W.M. Folkner, P.L. Bender, R.T. Stebbins

7. PERFORMING ORGANIZATION NAME(S) AND ADDRESS(ES)
Jet Propulsion Laboratory
California Institute of Technology
4800 Oak Grove Drive
Pasadena, CA 91109-8099

8. PERFORMING ORGANIZATION REPORT NUMBER
JPL Publication 97-16

9. SPONSORING / MONITORING AGENCY NAME(S) AND ADDRESS(ES)
National Aeronautics and Space Administration
Washington, DC 20546-0001

10. SPONSORING / MONITORING AGENCY REPORT NUMBER

11. SUPPLEMENTARY NOTES

12a. DISTRIBUTION / AVAILABILITY STATEMENT

12b. DISTRIBUTION CODE

13. ABSTRACT *(Maximum 200 words)*

This document presents the results of a design feasibility study for LISA (Laser Interferometer Space Antenna). The goal of LISA is to detect and study low-frequency astrophysical gravitational radiation from strongly relativistic regions. Astrophysical sources potentially visible to LISA include extra-galactic massive black hole binaries at cosmological distances, binary systems composed of a compact star and a massive black hole, galactic neutron star-black hole binaries, and background radiation from the Big Bang. The LISA mission will comprise three spacecraft located five million kilometers apart forming an equilateral triangle in an Earth-trailing orbit. Fluctuations in separation between shielded test masses located within each spacecraft will be determined by optical interferometry which determines the pase shift of laser light transmitted between the test masses.

14. SUBJECT TERMS
astrophysics, gravitational waves, interferometry, laser interferometer, LISA

15. NUMBER OF PAGES
87

16. PRICE CODE

17. SECURITY CLASSIFICATION OF REPORT	18. SECURITY CLASSIFICATION OF THIS PAGE	19. SECURITY CLASSIFICATION OF ABSTRACT	20. LIMITATION OF ABSTRACT
Unclassified	Unclassified	Unclassified	Unlimited